

# Time Series Compression using Quaternion Valued Neural Networks and Quaternion Backpropagation

Johannes Pöppelbaum and Andreas Schwung

**Abstract**—We propose a novel quaternionic time-series compression methodology where we divide a long time-series into segments of data, extract the min, max, mean and standard deviation of these chunks as representative features and encapsulate them in a quaternion, yielding a quaternion valued time-series. This time-series is processed using quaternion valued neural network layers, where we aim to preserve the relation between these features through the usage of the Hamilton product. To train this quaternion neural network, we derive quaternion backpropagation employing the GHR calculus, which is required for a valid product and chain rule in quaternion space. Furthermore, we investigate the connection between the derived update rules and automatic differentiation. We apply our proposed compression method on the Tennessee Eastman Dataset, where we perform fault classification using the compressed data in two settings: a fully supervised one and in a semi supervised, contrastive learning setting. Both times, we were able to outperform real valued counterparts as well as two baseline models: one with the uncompressed time-series as the input and the other with a regular downsampling using the mean. Further, we could improve the classification benchmark set by SimCLR-TS from 81.43% to 83.90%.

**Index Terms**—Quaternion Neural Network, Quaternion Backpropagation, Time-Series Compression, Fault Classification.

## I. INTRODUCTION

NOWADAYS, an extensive amount of time-series data is widely available, be it from industrial applications, Internet-of-Things (IoT) devices or wearables. Due to high sampling frequencies of sensors or long recording times, long sequences of data are the consequence. Often, the aim is to process them using machine learning models. However, this gets difficult as recurrent architectures might struggle with longer sequences as it is difficult to squeeze all seen information into a fixed length representation [1], [2].

Also, with more data to process, training times of models increase drastically. Likewise, storage requirements grow and potentially transmission times and energy consumption increases which is especially relevant for IoT devices. The authors of [3] show that a higher sampling rate as such did not increase the models accuracy while requiring significantly more training time when using a 1d-cnn based model architecture. Similarly, in [4] downsampling yielded performance improvements in a decoding task for multiple network architecture types.

Naturally, the question whether we can reduce the number of datapoints required for the machine learning task by applying a cheap to compute data compression arises. One common

used approach is piecewise aggregate approximation (PAA) [5] which divides a time series in  $N$  segments and takes the mean of the  $n$  datapoints included in  $N$  to form the compressed time series. It is popular for being very intuitive and easy and cheap to compute. However, this does not account for data deviations, as a sine wave with a high amplitude may later appear similar to a constant value. To overcome this downside and enrich the downsampled or compressed time-series with additional descriptive properties, we propose a novel, quaternion based time-compression method. In particular, we propose to divide a longer time-series into smaller chunks from which we extract four representative features, namely the min, max, mean and standard deviation. As this four properties are strongly related, we encapsulate them in the mathematical object of a quaternion. By utilizing the Hamilton product in quaternion valued one dimensional convolution layer, we aim to preserve their relationship during the feature extraction. While similar approaches have been proposed in the image domain [6], [7] where the r-, g- and b-channel of an image have been encoded in a quaternion, our approach is novel to the time-series domain, especially in combination with the quaternionic compression methodology. It can serve as an easy to implement improvement to already existing, PAA based implementations and pipelines without major refactoring, leveraging the strengths of quaternion valued neural network (QNN), namely relationship preservation and sparsity in comparison to a real valued equivalent.

Following the big success and broad range of applications of real-valued neural networks, in recent years along complex valued models [8]–[13] also quaternion valued models [6], [14]–[18] appealed the interest of researchers and gain more popularity over time. Applications are e.g. image tasks, 3D point cloud processing, speech / language tasks or sensor fusion. Quaternion valued MLPs using elementwise operating activation functions are further proven to be universal interpolators in  $\mathbb{H}$  [19]. To train these quaternion valued neural networks by means of gradient descent, [20]–[22] introduced quaternion backpropagation variants, using partial derivatives with respect to the four quaternion components. However, they do not use the GHR calculus [23], which is required for the validity of the product and chain rule in quaternion space (compare III-B1).

In this paper, after introducing the required quaternion algebra, we propose a novel quaternion backpropagation, based on the GHR calculus introduced in [23], considerably extending [24]. We provide implementation ready formulas for all parts of the computational chain including intermediate results. Furthermore, we propose a novel quaternion based time-series

compression and test it using the Tennessee Eastman (TE) dataset.

The main contributions of our work are the following:

- We propose a novel time-series compression method yielding a shorter, quaternion valued time-series. This compressed time-series is subsequently used for fault classification using a quaternion valued neural network model.
- We derive quaternion backpropagation using the GHR calculus which defines proper product and chain rules. We employ detailed calculations for each intermediate result, giving proper insights on the underlying quaternion mathematics.
- We investigate the relation of the derived quaternion backpropagation and automatic differentiation, revealing insights on scenarios where it can be used to train QNN.
- We experimentally prove the effectiveness of the proposed compression and provide detailed comparisons with real-valued counterparts as well as two baseline models in fully supervised learning setups. We further use a state of the art self-supervised learning setup to demonstrate that our approach outperforms previously set classification benchmarks.

The paper is structured as follows: Section II presents the related work and Section III the required fundamentals. Section IV continues with the derived quaternion valued backpropagation algorithm, Section V with the relation of quaternion backpropagation and automatic differentiation and Section VI with the proposed time-series compression methodology. Section VII provides the experimental evaluation. Finally, the paper is concluded by Section VIII.

## II. RELATED WORK

The related work can mainly be divided into the following categories: time-series compression, backpropagation techniques, especially in the complex or hypercomplex domain and finally applications of quaternion valued neural networks which are described in the following.

*Time-series Compression:* In the field of time-series data compression, it has to be separated between lossless and lossy compression techniques. The former is characterized by the fact that they allow for an error free reconstruction. Examples are SPRINTZ [25], DACTS [26], RAKE [27], RLBE [28] or DRH [29]. In contrast, the latter does not enable a perfect reconstruction, but instead allows for a higher compression rate as lossless techniques are limited in that regard. An often used lossy approach is to approximate the time-series using piece-wise linears [30]–[32] or polynomials [33]–[35]. Further approaches are e.g. SZ [36] or LFZip [37]. However, the compression approach is fundamentally different as it is not aiming for extracting representative features but instead uses approximations of the original data in a function representation. Furthermore, the focus here is usually on subsequent reconstruction rather than a fault classification using the compressed data.

The authors of [38] investigate the effect on the classification performance for univariate and multivariate time-series

data when applying compressed sensing, discrete wavelet transform (DWT), the SZ algorithm from [36] and a combination of DWT, lifting scheme and SZ as compression methods. In [39], the authors could show that by applying compressive sensing, the classification performance using a hidden Markov model for human activity recognition on video data could often be increased. Similarly, the authors of [40] were able to show that the use of a lossy compression does not reduce the prediction quality when using medical data to predict human stress levels using a multilayer perceptron (MLP) architecture. We differ from these works as we propose a quaternion based compression, intended for time-series data and to be processed with the Hamilton product within quaternion valued neural network (NN), for the first time. Furthermore, contrary to [38] and [40] we directly feed the compressed time-series data to the fault classification model instead of performing a reconstruction first and waive on utilizing the frequency domain as in the former.

Finally, [41] showed that PAA based approaches can benefit from additionally using the standard deviation rather than just the mean. Likewise, in [42] additionally to the mean, the minimum and maximum values are used. Our proposed methodology can be seen as the fusion of the two approaches within the quaternion space.

*Backpropagation:* The breakthrough of training neural networks using backpropagation started with the well known paper [43] and was extended and modified in a number of ways in the following. As neural networks emerged from the real numbers to the complex models, equivalent complex variants were introduced in [44]–[46]. A detailed description of the usage of the CR / Wirtinger Calculus, which comes in handy for complex backpropagation, can be found in [47]. None of them target quaternion valued models though. Related are also gradient based optimization techniques in the quaternion domain as described in [23], [48]. However, they differ from our work as they don't target multi-layered, perceptron based architectures.

Although, in contrast, these multi-layered, perceptron based architectures are targeted in [20]–[22], the respective used approaches suffer from the fact that the chain rule does not hold there. We overcome this by employing the GHR-Calculus and derive the quaternion backpropagation based on this, as initially proposed by [24], and significantly extend it.

*Application of Quaternion Neural Networks:* With regards to quaternion neural network applications, [6] composes fully quaternion valued models by combining quaternion convolution and quaternion fully-connected layers to use them on classification and denoising tasks of color images. Similarly, [49] uses quaternion valued variational autoencoders (VAEs) for image reconstruction and generation tasks, outperforming real valued VAEs while simultaneously reducing the number of parameters. The same observation was made by [50] when using quaternion generative adversarial networks (GAN) for image generation. The authors of [14] achieve rotational invariance for point-cloud inputs by utilizing quaternion valued inputs and features, the used weights and biases however are real valued matrices. In the context of speech/language understanding, [15] employs a quaternion MLP approach, where the

quaternion model could outperform real valued counterparts while requiring fewer epochs to be trained. Similarly, [16] utilizes quaternion convolutional neural networks (CNNs) and quaternion recurrent neural networks (RNNs) for this task. Again, these models were able to outperform their real-valued counterparts while requiring approximately four times fewer trainable parameters. In a related task, [51] employs quaternion CNN for emotion recognition in speech. In [17], a novel quaternion weight initialization strategies as well as quaternion batch-normalization is proposed to perform image classification and segmentation with quaternion valued models. A further application of recurrent quaternion models is [18] where quaternion RNNs, specifically Quaternion Gated Recurrent Units are applied on sensor fusion for navigation and human activity recognition. Finally, [52] proposes quaternion product units and uses them to human action and hand action recognition. Furthermore, they utilize them for point cloud classification. All these mentioned approaches differ from our work as none is concerned with time series compression of industrial data in the quaternion domain, in particular with a fault classification downstream task where the compressed data serves as the models input.

### III. FUNDAMENTALS

This section introduces the required fundamentals, starting with the mathematics of quaternions, followed by quaternion derivatives and the regular backpropagation algorithm for real valued neural networks.

#### A. Quaternions

1) *Quaternion Algebra*: Quaternions were discovered by Hamilton in 1843 [53] as a method to extend the complex numbers to the three dimensional space. A quaternion  $q, q \in \mathbb{H}$  consists of three parts, one real and three imaginary

$$q = q_0 + q_1i + q_2j + q_3k = q_0 + \mathbf{q}$$

where  $q_0, q_1, q_2, q_3 \in \mathbb{R}$ . Often,  $q_0$  is referred to as the real part and  $\mathbf{q}$  as the vector part. The imaginary components  $i, j, k$  have the properties

$$\begin{aligned} i^2 = j^2 = k^2 = ijk = -1 \\ ij = +k, \quad jk = +i, \quad ki = +j \\ ji = -k, \quad kj = -i, \quad ik = -j. \end{aligned}$$

Similar to complex numbers, quaternions have a conjugate:

$$q^* = q_0 - q_1i - q_2j - q_3k = q_0 - \mathbf{q}$$

A quaternion  $q$  fulfilling  $\|q\| = \sqrt{qq^*} = \sqrt{q_0^2 + q_1^2 + q_2^2 + q_3^2} = 1$  is called a unit quaternion and a quaternion  $q$  with  $q_0 = 0$  is called a pure quaternion.

The addition of two quaternions  $x, y$  is defined as

$$x + y = (x_0 + y_0) + (x_1 + y_1)i + (x_2 + y_2)j + (x_3 + y_3)k$$

and multiplication as

$$\begin{aligned} x \otimes y &= x_0y_0 - \mathbf{x} \cdot \mathbf{y} + x_0\mathbf{y} + y_0\mathbf{x} + \mathbf{x} \times \mathbf{y} \\ &= (x_0y_0 - x_1y_1 - x_2y_2 - x_3y_3) \\ &\quad + (x_0y_1 + x_1y_0 + x_2y_3 - x_3y_2)i \\ &\quad + (x_0y_2 - x_1y_3 + x_2y_0 + x_3y_1)j \\ &\quad + (x_0y_3 + x_1y_2 - x_2y_1 + x_3y_0)k. \end{aligned} \quad (1)$$

We further define the quaternion Hadamard-product of two quaternions  $x, y$  as

$$x \circ y = x_0y_0 + x_1y_1i + x_2y_2j + x_3y_3k.$$

2) *Quaternion Involutions*: Of particular importance for the quaternion derivatives are the quaternion self-inverse mappings or involutions, defined as [54]

$$\phi(\eta) = q^\eta = \eta q \eta^{-1} = \eta q \eta^* = -\eta q \eta \quad (2)$$

where  $\eta$  is a pure unit quaternion. Using Equation (2), we can create the involutions as

$$\begin{aligned} q &= q_0 + q_1i + q_2j + q_3k \\ q^i &= -iqi = q_0 + q_1i - q_2j - q_3k \\ q^j &= -jqj = q_0 - q_1i + q_2j - q_3k \\ q^k &= -kqk = q_0 - q_1i - q_2j + q_3k. \end{aligned}$$

The corresponding conjugate involutions are

$$\begin{aligned} q^{i*} &= q_0 - q_1i + q_2j + q_3k \\ q^{j*} &= q_0 + q_1i - q_2j + q_3k \\ q^{k*} &= q_0 + q_1i + q_2j - q_3k. \end{aligned}$$

With their help, various relations can be created which come in handy in the following quaternion valued derivation calculations, as they often help in simplifying the calculations and to avoid elaborate term sorting [23], [55]:

$$\begin{aligned} q_0 &= \frac{1}{4} (q + q^i + q^j + q^k), \quad q_1 = -\frac{i}{4} (q + q^i - q^j - q^k) \\ q_2 &= -\frac{j}{4} (q - q^i + q^j - q^k), \quad q_3 = -\frac{k}{4} (q - q^i - q^j + q^k) \end{aligned} \quad (3)$$

$$\begin{aligned} q_0 &= \frac{1}{4} (q^* + q^{i*} + q^{j*} + q^{k*}), \quad q_1 = \frac{i}{4} (q^* + q^{i*} - q^{j*} - q^{k*}) \\ q_2 &= \frac{j}{4} (q^* - q^{i*} + q^{j*} - q^{k*}), \quad q_3 = \frac{k}{4} (q^* - q^{i*} - q^{j*} + q^{k*}) \end{aligned} \quad (4)$$

$$\begin{aligned} q^* &= \frac{1}{2} (-q + q^i + q^j + q^k), \quad q^{i*} = \frac{1}{2} (q - q^i + q^j + q^k) \\ q^{j*} &= \frac{1}{2} (q + q^i - q^j + q^k), \quad q^{k*} = \frac{1}{2} (q + q^i + q^j - q^k) \end{aligned} \quad (5)$$

$$\begin{aligned} q &= \frac{1}{2} (-q^* + q^{i*} + q^{j*} + q^{k*}), \quad q^i = \frac{1}{2} (q^* - q^{i*} + q^{j*} + q^{k*}) \\ q^j &= \frac{1}{2} (q^* + q^{i*} - q^{j*} + q^{k*}), \quad q^k = \frac{1}{2} (q^* + q^{i*} + q^{j*} - q^{k*}) \end{aligned} \quad (6)$$

## B. Quaternion Derivatives

1) *Partial derivatives:* For a quaternion valued function  $f(q), q = q_0 + q_1i + q_2j + q_3k$ , [20] and [21] calculate the derivatives as follows:

$$\frac{\partial f}{\partial q} = \left( \frac{\partial f}{\partial q_0} + \frac{\partial f}{\partial q_1}i + \frac{\partial f}{\partial q_2}j + \frac{\partial f}{\partial q_3}k \right) \quad (7)$$

However, as we will show now, neither the product rule nor the chain rule hold for this approach.

**Proposition 1.** *For the derivative of a quaternion valued function  $f(q), q \in \mathbb{H}$  following (7), the product rule does not hold.*

*Proof.* Consider  $f(q) = qq^* = q_0^2 + q_1^2 + q_2^2 + q_3^2$  as the function of choice. The direct derivation following (7) yields

$$\begin{aligned} \frac{\partial f}{\partial q} &= \left( \frac{\partial f}{\partial q_0} + \frac{\partial f}{\partial q_1}i + \frac{\partial f}{\partial q_2}j + \frac{\partial f}{\partial q_3}k \right) \\ &= (2q_0 + 2q_1i + 2q_2j + 2q_3k) = 2q \end{aligned}$$

Using the product rule, we can calculate the same derivation using

$$\begin{aligned} \frac{\partial}{\partial q}(qq^*) &= q \frac{\partial q^*}{\partial q} + \frac{\partial q}{\partial q} q^* \\ &= q \frac{\partial}{\partial q}(q_0 - q_1i - q_2j - q_3k) \\ &\quad + \frac{\partial}{\partial q}(q_0 + q_1i + q_2j + q_3k) q^* \\ &= q(1 - ii - jj - kk) + (1 + ii + jj + kk) q^* \\ &= 4q - 2q^* \neq 2q. \end{aligned} \quad \square$$

**Proposition 2.** *For the derivative of a quaternion valued function  $f(\zeta(x, y)); x, y, \zeta \in \mathbb{H}$  following (7), the chain rule does not hold.*

*Proof.* Consider  $f(q) = \zeta\zeta^*; \zeta = xy$  as the function of choice.

We start by calculating the derivative without the chain rule:

$$\begin{aligned} \frac{\partial f}{\partial x} &= \frac{\partial}{\partial x} \left[ (xy)(xy)^* \right] \\ &= \frac{\partial}{\partial x} \left[ (x_0 + x_1i + x_2j + x_3k)(y_0 + y_1i + y_2j + y_3k) \right. \\ &\quad \left. (y_0 - y_1i - y_2j - y_3k)(x_0 - x_1i - x_2j - x_3k) \right] \\ &= \frac{\partial}{\partial x} \left[ x_0^2y_0^2 + x_0^2y_1^2 + x_0^2y_2^2 + x_0^2y_3^2 \right. \\ &\quad \left. + x_1^2y_0^2 + x_1^2y_1^2 + x_1^2y_2^2 + x_1^2y_3^2 + x_2^2y_0^2 + x_2^2y_1^2 \right. \\ &\quad \left. + x_2^2y_2^2 + x_2^2y_3^2 + x_3^2y_0^2 + x_3^2y_1^2 + x_3^2y_2^2 + x_3^2y_3^2 \right] \\ &= 2x_0y_0^2 + 2x_0y_1^2 + 2x_0y_2^2 + 2x_0y_3^2 \\ &\quad + (2x_1y_0^2 + 2x_1y_1^2 + 2x_1y_2^2 + 2x_1y_3^2) i \\ &\quad + (2x_2y_0^2 + 2x_2y_1^2 + 2x_2y_2^2 + 2x_2y_3^2) j \\ &\quad + (2x_3y_0^2 + 2x_3y_1^2 + 2x_3y_2^2 + 2x_3y_3^2) k \end{aligned}$$

Using the chain rule  $\frac{\partial f}{\partial x} = \frac{\partial f}{\partial \zeta} \frac{\partial \zeta}{\partial x}$ , the outer derivative yields

$$\begin{aligned} \frac{\partial f}{\partial \zeta} &= \frac{\partial}{\partial \zeta} (\zeta\zeta^*) = \frac{\partial}{\partial \zeta} (z_0^2 + z_1^2 + z_2^2 + z_3^2) \\ &= 2(z_0 + z_1i + z_2j + z_3k) = 2\zeta \end{aligned}$$

and the inner derivative is

$$\begin{aligned} \frac{\partial \zeta}{\partial x} &= \frac{\partial}{\partial x} (xy) = \frac{\partial}{\partial x} (x_0y_0 + x_0y_1i + x_0y_2j + x_0y_3k \\ &\quad + x_1y_0i - x_1y_1 + x_1y_2k - x_1y_3j + x_2y_0j - x_2y_1k \\ &\quad - x_2y_2 + x_2y_3i + x_3y_0k + x_3y_1j - x_3y_2i - x_3y_3) \\ &= 2(-y_0 + y_1i + y_2j + y_3)k = -2y^*. \end{aligned}$$

Combining inner and outer derivative yields

$$\begin{aligned} \frac{\partial f}{\partial x} &= \frac{\partial f}{\partial \zeta} \frac{\partial \zeta}{\partial x} = 2\zeta(-2y^*) = -4(xy y^*) \\ &= -4x_0y_0^2 - 4x_0y_1^2 - 4x_0y_2^2 - 4x_0y_3^2 \\ &\quad + (-4x_1y_0^2 - 4x_1y_1^2 - 4x_1y_2^2 - 4x_1y_3^2) i \\ &\quad + (-4x_2y_0^2 - 4x_2y_1^2 - 4x_2y_2^2 - 4x_2y_3^2) j \\ &\quad + (-4x_3y_0^2 - 4x_3y_1^2 - 4x_3y_2^2 - 4x_3y_3^2) k \end{aligned}$$

Obviously the results don't match up and hence chain rule does not hold for this way of calculating quaternion derivatives.  $\square$

2) *GHR-Calculus:* Initial improvements on Quaternion Derivatives yielded the HR-Calculus, however it still lacks the validity of the product- and chain-rule (Compare Appendix A). Hence, [23] extends it to the GHR-Calculus, enabling the definition of a novel quaternion product- and chain-rule. The derivative and conjugate derivative are defined as

$$\frac{\partial f}{\partial q^\mu} = \frac{1}{4} \left( \frac{\partial f}{\partial q_0} - \frac{\partial f}{\partial q_1}i^\mu - \frac{\partial f}{\partial q_2}j^\mu - \frac{\partial f}{\partial q_3}k^\mu \right) \quad (8)$$

$$\frac{\partial f}{\partial q^{\mu*}} = \frac{1}{4} \left( \frac{\partial f}{\partial q_0} + \frac{\partial f}{\partial q_1}i^\mu + \frac{\partial f}{\partial q_2}j^\mu + \frac{\partial f}{\partial q_3}k^\mu \right) \quad (9)$$

whereby  $\mu \neq 0, \mu \in \mathbb{H}$ .

a) *The Conjugate Rule:* For a real valued function  $f$ , [23] define the conjugate rule as

$$\left( \frac{\partial f}{\partial q^\mu} \right)^* = \frac{\partial f}{\partial q^{\mu*}}, \quad \left( \frac{\partial f}{\partial q^{\mu*}} \right)^* = \frac{\partial f}{\partial q^\mu} \quad (10)$$

b) *The Product Rule:* Furthermore, they define the quaternion product rule as

$$\frac{\partial(fg)}{\partial q^\mu} = f \frac{\partial(g)}{\partial q^\mu} + \frac{\partial(f)}{\partial q^{\mu*}} g, \quad \frac{\partial(fg)}{\partial q^{\mu*}} = f \frac{\partial(g)}{\partial q^{\mu*}} + \frac{\partial(f)}{\partial q^{\mu*}} g.$$

c) *The Chain Rule:* Finally, [23] also defines a quaternion chain rule as

$$\begin{aligned} \frac{\partial f(g(q))}{\partial q^\mu} &= \frac{\partial f}{\partial g^\nu} \frac{\partial g^\nu}{\partial q^\mu} + \frac{\partial f}{\partial g^{\nu i}} \frac{\partial g^{\nu i}}{\partial q^\mu} + \frac{\partial f}{\partial g^{\nu j}} \frac{\partial g^{\nu j}}{\partial q^\mu} + \frac{\partial f}{\partial g^{\nu k}} \frac{\partial g^{\nu k}}{\partial q^\mu} \\ \frac{\partial f(g(q))}{\partial q^{\mu*}} &= \frac{\partial f}{\partial g^\nu} \frac{\partial g^\nu}{\partial q^{\mu*}} + \frac{\partial f}{\partial g^{\nu i}} \frac{\partial g^{\nu i}}{\partial q^{\mu*}} + \frac{\partial f}{\partial g^{\nu j}} \frac{\partial g^{\nu j}}{\partial q^{\mu*}} + \frac{\partial f}{\partial g^{\nu k}} \frac{\partial g^{\nu k}}{\partial q^{\mu*}} \end{aligned}$$

with  $\mu, \nu \in \mathbb{H}$ ,  $\mu\nu \neq 0$ .

Note that unless otherwise stated, in the following we always use  $\mu = \nu = 1+0i+0j+0k$  as this simplifies the notation throughout the calculations. For further understanding, detailed example calculations can be found in the Appendix B.

#### IV. QUATERNION BACKPROPAGATION

In this section, we derive the backpropagation for QNNs based on the GHR-Calculus. We start by defining the forward phase and the quaternary loss function, then the derivation of the actual backpropagation follows. Specifically, we start with the derivatives of the final layer of a QNN and work our way backwards through the architecture and continue with deriving the derivatives for an arbitrary hidden layer, following the usual backpropagation order of sequence.

##### A. Forward phase and Loss function

We can formulate the forward phase of a regular feed-forward QNN layer ( $l$ ) with  $n$  inputs and  $m$  outputs as follows:

$$a_i^{(l)} = \sigma(\zeta_i^{(l)}), \quad \zeta_i^{(l)} = \sum_{j=1}^n w_{i,j}^{(l)} a_j^{(l-1)} + \beta_i^{(l)}$$

where  $i \in \{1, \dots, m\}$ ,  $j \in \{1, \dots, n\}$  and  $w, y, \beta, a, \zeta \in \mathbb{H}$ . The corresponding matrix-vector formulation is

$$\mathbf{a}^{(l)} = \sigma(\boldsymbol{\zeta}^{(l)}), \quad \boldsymbol{\zeta}^{(l)} = \mathcal{W}^{(l)} \mathbf{a}^{(l-1)} + \boldsymbol{\beta}^{(l)} \quad (11)$$

where  $\mathcal{W} \in \mathbb{H}^{m \times n}$  and  $\boldsymbol{\beta} \in \mathbb{H}^m$ . The final output  $\mathbf{y} \in \mathbb{H}^m$  of the last layer  $L$  and hence the overall model is  $\mathbf{a}^{(L)}$ .

We define the loss function  $\mathcal{L}(\cdot)$  between the desired output  $d_i$  and the actual output  $y_i$  as

$$\mathcal{L} = \mathbf{e}^{*T} \mathbf{e}$$

whereby  $e_i \in \{1, \dots, m\}$  and  $e_i = d_i - y_i$ . By doing so, we obtain the real valued loss

$$\begin{aligned} \mathcal{L} &= e_1^* e_1 + e_2^* e_2 + \dots + e_m^* e_m \\ &= (e_{01}^2 + e_{11}^2 + e_{21}^2 + e_{31}^2) + (e_{02}^2 + e_{12}^2 + e_{22}^2 + e_{32}^2) \\ &\quad + \dots + (e_{0m}^2 + e_{1m}^2 + e_{2m}^2 + e_{3m}^2) \\ &= (d_{01} - y_{01})^2 + (d_{11} - y_{11})^2 \\ &\quad + (d_{21} - y_{21})^2 + (d_{31} - y_{31})^2 \\ &\quad + (d_{02} - y_{02})^2 + (d_{12} - y_{12})^2 \\ &\quad + (d_{22} - y_{22})^2 + (d_{32} - y_{32})^2 \\ &\quad + \dots \\ &\quad + (d_{0m} - y_{0m})^2 + (d_{1m} - y_{1m})^2 \\ &\quad + (d_{2m} - y_{2m})^2 + (d_{3m} - y_{3m})^2. \end{aligned} \quad (12)$$

##### B. Final layer

We start deriving the quaternion backpropagation algorithm by first considering the output of the final layer of a QNN without the usage of an activation function. If an activation function shall be used, one can use intermediate results and

apply the strategy from the following Subsection IV-C. Recalling Equation (11), the output  $\mathbf{y}$  of a QNN is calculated as

$$\mathbf{y} = \mathcal{W}^{(L)} \mathbf{a}^{(L-1)} + \boldsymbol{\beta}^{(L)}$$

where  $\mathbf{a}^{(L-1)}$  is the output of the previous layer. One output quaternion  $y_i$  can be obtained using

$$y_i = \sum_{j=1}^n w_{i,j}^{(L)} a_j^{(L-1)} + \beta_i^{(L)}.$$

For deriving  $\mathcal{L}$  with respect to the weights  $\mathcal{W}^{(L)}$ , biases  $\boldsymbol{\beta}^{(L)}$  and activation outputs of the previous layer  $\mathbf{a}^{(L-1)}$ , we utilize the chain rule where we first derive  $\frac{\partial \mathcal{L}}{\partial \mathbf{y}}$  and then  $\frac{\partial \mathbf{y}}{\partial \mathcal{W}^*}$ ,  $\frac{\partial \mathbf{y}}{\partial \boldsymbol{\beta}^*}$  and  $\frac{\partial \mathbf{y}}{\partial \mathbf{a}}$ .

Note that we use the conjugate  $\mathcal{W}^*$  and  $\boldsymbol{\beta}^*$  as this is the direction of the steepest descent [23], [48]. For better readability, we waive on the subscripts  $\square_{i,j}$  indicating the matrix/vector elements as well as the superscript  $\square^{(L)}$  throughout the following calculations.

##### 1) Derivative with respect to the weights:

**Theorem 1.** *The derivative of  $\mathcal{L}$  with respect to the weights  $w_{i,j}^{(L)}$  of a QNN is*

$$\frac{\partial \mathcal{L}(y(w, \beta))}{\partial w^*} = -\frac{1}{2} e a^* = -\frac{1}{2} (d - y) a^*.$$

*Proof.* The derivative with respect to the weights  $w_{i,j}^{(L)}$  following the GHR-Calculus is calculated as follows:

$$\frac{\partial \mathcal{L}(y(w, \beta))}{\partial w^*} = \frac{\partial \mathcal{L}}{\partial y} \frac{\partial y}{\partial w^*} + \frac{\partial \mathcal{L}}{\partial y^i} \frac{\partial y^i}{\partial w^*} + \frac{\partial \mathcal{L}}{\partial y^j} \frac{\partial y^j}{\partial w^*} + \frac{\partial \mathcal{L}}{\partial y^k} \frac{\partial y^k}{\partial w^*}.$$

We start by calculating the respective left partial derivatives

$$\begin{aligned} \frac{\partial \mathcal{L}}{\partial y} &= \frac{\partial}{\partial y} [(d_0 - y_0)^2 + (d_1 - y_1)^2 + (d_2 - y_2)^2 + (d_3 - y_3)^2] \\ &= \frac{1}{4} [-2(d_0 - y_0) + 2(d_1 - y_1)i + 2(d_2 - y_2)j + 2(d_3 - y_3)k] \\ &= -\frac{1}{2} [(d_0 - y_0) - (d_1 - y_1)i - (d_2 - y_2)j - (d_3 - y_3)k] \\ &= -\frac{1}{2} (d - y)^* = -\frac{1}{2} e^* \end{aligned} \quad (13)$$

For the derivatives with respect to the involutions  $y^i$ ,  $y^j$  and  $y^k$  we just state the final results here, the detailed calculations can be found in the Appendix C-A.

$$\frac{\partial \mathcal{L}}{\partial y^i} = -\frac{1}{2} (d - y)^{i*} = -\frac{1}{2} e^{i*}$$

$$\frac{\partial \mathcal{L}}{\partial y^j} = -\frac{1}{2} (d - y)^{j*} = -\frac{1}{2} e^{j*}$$

$$\frac{\partial \mathcal{L}}{\partial y^k} = -\frac{1}{2} (d - y)^{k*} = -\frac{1}{2} e^{k*} \quad (14)$$

Now we calculate the right partial derivatives of  $y$ ,  $y^i$ ,  $y^j$  and  $y^k$  with respect to  $w^*$ :

$$\begin{aligned}
\frac{\partial y}{\partial \omega^*} &= \frac{\partial(\omega a + \beta)}{\partial \omega^*} = \frac{\partial(\omega a)}{\partial \omega^*} \\
&= \frac{\partial}{\partial \omega^*} [(a_0 w_0 - a_1 w_1 - a_2 w_2 - a_3 w_3) \\
&\quad + (a_0 w_1 + a_1 w_0 - a_2 w_3 + a_3 w_2) i \\
&\quad + (a_0 w_2 + a_1 w_3 + a_2 w_0 - a_3 w_1) j \\
&\quad + (a_0 w_3 - a_1 w_2 + a_2 w_1 + a_3 w_0) k] \\
&= \frac{1}{4} [a_0 + a_1 i + a_2 j + a_3 k + (a_0 i - a_1 + a_2 k - a_3 j) i \\
&\quad + (a_0 j - a_1 k - a_2 + a_3 i) j + (a_0 k + a_1 j - a_2 i - a_3) k] \\
&= \frac{1}{2} [-a_0 + a_1 + a_2 + a_3] = -\frac{1}{2} a^*
\end{aligned} \tag{15}$$

For the involutions, again we just state the final results, the detailed calculations can be found in the Appendix C-B.

$$\frac{\partial y^i}{\partial \omega^*} = \frac{\partial y^j}{\partial \omega^*} = \frac{\partial y^k}{\partial \omega^*} = \frac{1}{2} a^* \tag{16}$$

Combining both parts to form the overall derivative yields

$$\begin{aligned}
\frac{\partial \mathcal{L}(y(\omega, \beta))}{\partial \omega^*} &= \frac{-1}{2} e^* \frac{-1}{2} a^* + \frac{-1}{2} e^{i*} \frac{1}{2} a^* \\
&\quad + \frac{-1}{2} e^{j*} \frac{1}{2} a^* + \frac{-1}{2} e^{k*} \frac{1}{2} a^* \\
&= \frac{1}{4} [e^* - e^{i*} - e^{j*} - e^{k*}] a^* \stackrel{(6)}{=} -\frac{1}{2} e a^*
\end{aligned} \tag{17}$$

which concludes the proof  $\square$

2) *Derivative with respect to the bias:* Likewise, we need to derive  $\mathcal{L}$  with respect to the bias  $\beta_i^{(L)}$ .

**Theorem 2.** *The derivative of  $\mathcal{L}$  with respect to the bias  $\beta_i^{(L)}$  of a QNN is*

$$\frac{\partial \mathcal{L}(y(\omega, \beta))}{\partial \beta^*} = -\frac{1}{2} e = -\frac{1}{2} (d - y).$$

*Proof.* Similarly to the weights, the derivative is defined as follows:

$$\frac{\partial \mathcal{L}(y(\omega, \beta))}{\partial \beta^*} = \frac{\partial \mathcal{L}}{\partial y} \frac{\partial y}{\partial \beta^*} + \frac{\partial \mathcal{L}}{\partial y^i} \frac{\partial y^i}{\partial \beta^*} + \frac{\partial \mathcal{L}}{\partial y^j} \frac{\partial y^j}{\partial \beta^*} + \frac{\partial \mathcal{L}}{\partial y^k} \frac{\partial y^k}{\partial \beta^*}.$$

The left partial derivatives are already known from Equations (13) - (14) in IV-B1, hence we just have to calculate the right partial derivatives:

$$\begin{aligned}
\frac{\partial y}{\partial \beta^*} &= \frac{\partial(\omega a + \beta)}{\partial \beta^*} = \frac{\partial(\beta)}{\partial \beta^*} \\
&= \frac{\partial}{\partial \beta^*} (b_0 + b_1 i + b_2 j + b_3 k) \\
&= \frac{1}{4} (1 + ii + jj + kk) = -0.5
\end{aligned} \tag{18}$$

For the three involutions  $y^i$ ,  $y^j$  and  $y^k$ , the detailed calculations can be found in the Appendix C-C and we just state the results here:

$$\frac{\partial y^i}{\partial \beta^*} = \frac{\partial y^j}{\partial \beta^*} = \frac{\partial y^k}{\partial \beta^*} = 0.5 \tag{19}$$

Combining the left and right partial derivatives is related to Equation (17) with the exception that the right derivatives are missing the  $a^*$ . Consequently, the final derivative is

$$\frac{\partial \mathcal{L}(e(\omega, \beta))}{\partial \beta^*} = -\frac{1}{2} e. \quad \square$$

3) *Derivative with respect to activations:* Finally, we need to derive the loss with respect to the activations / outputs of the previous layer  $a_j^{(L-1)}$ .

**Theorem 3.** *The derivative of  $\mathcal{L}$  with respect to the activations  $a_j^{(L-1)}$  of a QNN yields*

$$\frac{\partial \mathcal{L}(a_j^{(L-1)})}{\partial a_j^{(L-1)}} = \sum_{i \in K} -\frac{1}{2} e_i^* w_{i,j}.$$

*Proof.* As multiple output neurons  $i \in K$  are connected to  $a_j^{(L-1)}$ , we have to take the sum of the respective derivatives:

$$\begin{aligned}
\frac{\partial \mathcal{L}(a_j^{(L-1)})}{\partial a_j^{(L-1)}} &= \sum_{i \in K} \frac{\partial \mathcal{L}(y_i^{(l)}(a_j^{(L-1)}))}{\partial a_j^{(L-1)}} \\
&= \sum_{i \in K} \frac{\partial \mathcal{L}}{\partial y_i} \frac{\partial y_i}{\partial a_j} + \frac{\partial \mathcal{L}}{\partial y_i^i} \frac{\partial y_i^i}{\partial a_j} + \frac{\partial \mathcal{L}}{\partial y_i^j} \frac{\partial y_i^j}{\partial a_j} + \frac{\partial \mathcal{L}}{\partial y_i^k} \frac{\partial y_i^k}{\partial a_j}
\end{aligned}$$

The calculations for the individual parts of the sum are analog to the ones when deriving with respect to the weights, hence we will not list the detailed calculations here but report the results. The detailed derivatives can be found in the Appendix C-D.

$$\begin{aligned}
\frac{\partial y}{\partial a} &= \frac{\partial(\omega a + \beta)}{\partial a} = \omega, & \frac{\partial y^i}{\partial a} &= \frac{\partial(\omega a + \beta)^i}{\partial a} = 0 \\
\frac{\partial y^j}{\partial a} &= \frac{\partial(\omega a + \beta)^j}{\partial a} = 0, & \frac{\partial y^k}{\partial a} &= \frac{\partial(\omega a + \beta)^k}{\partial a} = 0
\end{aligned} \tag{20}$$

Finally, the derivative formulates as

$$\frac{\partial \mathcal{L}(a_j)}{\partial a_j} = \sum_{i \in K} -\frac{1}{2} e_i^* w_{i,j}.$$

which concludes the proof.  $\square$

In the same manner, we can obtain the derivatives

$$\begin{aligned}
\frac{\partial \mathcal{L}(a_j)}{\partial a_j^i} &= \sum_{i \in K} -\frac{1}{2} (e_i^* w_{i,j})^i \\
\frac{\partial \mathcal{L}(a_j)}{\partial a_j^j} &= \sum_{i \in K} -\frac{1}{2} (e_i^* w_{i,j})^j \\
\frac{\partial \mathcal{L}(a_j)}{\partial a_j^k} &= \sum_{i \in K} -\frac{1}{2} (e_i^* w_{i,j})^k
\end{aligned} \tag{21}$$

which we need for applying the chain rule.

4) *Update rules for the last layer:* Based on the previous calculations, the update rules of weights and biases at timestep  $n$  for the last layer are

$$\begin{aligned} \omega_{i,j}^{(L)}(n+1) &= \omega_{i,j}^{(L)}(n) - \lambda \frac{1}{2} e_i(n) a_j^{*(L-1)}(n) \\ \beta_i^{(L)}(n+1) &= \beta_i^{(L)}(n) - \lambda \frac{1}{2} e_i(n) \end{aligned}$$

whereby  $\lambda$  indicates the learning rate.

### C. Hidden layer

For the hidden layers, usually activation functions are used. Thus, we obtain three parts we have to derive for. As we know already from the quaternion chain rule, we cannot simply combine them multiplicatively, especially for the three components. Instead, we first start with deriving with respect to the activation input, where the loss is a function

$$\mathcal{L}(a^{(l)}) = \mathcal{L}\left(a^{(l)}\left(\tilde{z}^{(l)}\right)\right); a^{(l)} = \sigma\left(\tilde{z}^{(l)}\right).$$

Then, we can create the involutions of this derivative and continue with deriving with respect to  $\omega_{i,j}^{(l)}$ ,  $\beta_i^{(l)}$  and  $a_i^{(l-1)}$ . For simplicity and better readability, we will avoid the superscript  $\square^{(l)}$  indicating the layer when we deal with the involutions to prevent double superscripts.

#### 1) Derivative with respect to the activation input:

**Theorem 4.** *The derivative of  $\mathcal{L}$  with respect to the activation input  $\tilde{z}_i^{(l)}$  of a QNN is*

$$\begin{aligned} \frac{\partial \mathcal{L}}{\partial \tilde{z}_i^{(l)}} &= p_0 \sigma'(z_0) + p_1 \sigma'(z_1)i + p_2 \sigma'(z_2)j + p_3 \sigma'(z_3)k \\ &= \rho \circ \sigma'(\tilde{z}) \end{aligned}$$

whereby  $\rho$  is the derivative of the next layer and  $\sigma(\cdot)$  is an elementwise activation function.

*Proof.* For deriving with respect to the activation input  $\tilde{z}_i^{(l)}$  we have to calculate

$$\frac{\partial \mathcal{L}(a^{(l)}(\tilde{z}^{(l)}))}{\partial \tilde{z}_i^{(l)}} = \frac{\partial \mathcal{L}}{\partial a} \frac{\partial a}{\partial \tilde{z}} + \frac{\partial \mathcal{L}}{\partial a^i} \frac{\partial a^i}{\partial \tilde{z}} + \frac{\partial \mathcal{L}}{\partial a^j} \frac{\partial a^j}{\partial \tilde{z}} + \frac{\partial \mathcal{L}}{\partial a^k} \frac{\partial a^k}{\partial \tilde{z}}.$$

We can derive the outer equation with respect to both, the regular quaternion or it's conjugate, and here it's more convenient and simultaneously also computationally more efficient to choose the regular quaternion as  $\tilde{z}$  is a direct result of the forward phase while  $\tilde{z}^*$  is not.

To obtain the derivatives with respect to the involutions  $a^i$ ,  $a^j$  and  $a^k$  we can simply take the known result and flip the signs of the imaginary parts according to Equation (24). For the last layer we know  $\frac{\partial \mathcal{L}}{\partial a}$  already. For an arbitrary hidden layer ( $l$ ) we don't know it yet. Hence, for better readability and generalization, in the following we will call the result simply  $\rho^{(l+1)}$ . As this is coming from the following layer we assign the superscript  $\square^{(l+1)}$ . Furthermore, this naming is also convenient since the result will change from the last layer to the hidden layer, but we can always refer to it as  $\rho$ .

For the right part of the partial derivatives, we first need to obtain the derivatives of  $a(z)$  and it's involutions

$a^i(z)$ ,  $a^j(z)$  and  $a^k(z)$ . Using an element-wise operating activation function  $\sigma(\cdot)$  to calculate  $a^{(l)} = \sigma(\tilde{z}) = \sigma(z_0) + \sigma(z_1)i + \sigma(z_2)j + \sigma(z_3)k$  these are

$$\begin{aligned} \frac{\partial a}{\partial \tilde{z}} &= \frac{\partial}{\partial \tilde{z}} [\sigma(z_0) + \sigma(z_1)i + \sigma(z_2)j + \sigma(z_3)k] \\ &= \frac{1}{4} [\sigma'(z_0) + \sigma'(z_1) + \sigma'(z_2) + \sigma'(z_3)] \end{aligned}$$

$$\begin{aligned} \frac{\partial a^i}{\partial \tilde{z}} &= \frac{\partial}{\partial \tilde{z}} [\sigma(z_0) + \sigma(z_1)i - \sigma(z_2)j - \sigma(z_3)k] \\ &= \frac{1}{4} [\sigma'(z_0) + \sigma'(z_1) - \sigma'(z_2) - \sigma'(z_3)] \end{aligned}$$

$$\begin{aligned} \frac{\partial a^j}{\partial \tilde{z}} &= \frac{\partial}{\partial \tilde{z}} [\sigma(z_0) - \sigma(z_1)i + \sigma(z_2)j - \sigma(z_3)k] \\ &= \frac{1}{4} [\sigma'(z_0) - \sigma'(z_1) + \sigma'(z_2) - \sigma'(z_3)] \end{aligned}$$

$$\begin{aligned} \frac{\partial a^k}{\partial \tilde{z}} &= \frac{\partial}{\partial \tilde{z}} [\sigma(z_0) - \sigma(z_1)i - \sigma(z_2)j + \sigma(z_3)k] \\ &= \frac{1}{4} [\sigma'(z_0) - \sigma'(z_1) - \sigma'(z_2) + \sigma'(z_3)] \end{aligned}$$

Combining the respective partial derivatives yields

$$\begin{aligned} \frac{\partial \mathcal{L}}{\partial z^{(l)}} &= \frac{\partial \mathcal{L}(a^{(l)}(z^{(l)}))}{\partial z^{(l)}} \\ &= \rho \frac{1}{4} [\sigma'(z_0) + \sigma'(z_1) + \sigma'(z_2) + \sigma'(z_3)] \\ &\quad + \rho^i \frac{1}{4} [\sigma'(z_0) + \sigma'(z_1) - \sigma'(z_2) - \sigma'(z_3)] \\ &\quad + \rho^j \frac{1}{4} [\sigma'(z_0) - \sigma'(z_1) + \sigma'(z_2) - \sigma'(z_3)] \\ &\quad + \rho^k \frac{1}{4} [\sigma'(z_0) - \sigma'(z_1) - \sigma'(z_2) + \sigma'(z_3)] \\ &= \frac{1}{4} [\rho + \rho^i + \rho^j + \rho^k] \sigma'(z_0) \\ &\quad + \frac{1}{4} [\rho + \rho^i - \rho^j - \rho^k] \sigma'(z_1) \\ &\quad + \frac{1}{4} [\rho - \rho^i + \rho^j - \rho^k] \sigma'(z_2) \\ &\quad + \frac{1}{4} [\rho - \rho^i - \rho^j + \rho^k] \sigma'(z_3) \\ &= p_0 \sigma'(z_0) + p_1 \sigma'(z_1)i + p_2 \sigma'(z_2)j + p_3 \sigma'(z_3)k \\ &= \rho \circ \sigma'(\tilde{z}) \end{aligned}$$

which concludes the proof.  $\square$

Note that in the last step we used the alternative representations

$$\begin{aligned} q_0 &= \frac{1}{4} (q + q^i + q^j + q^k), & q_1 i &= \frac{1}{4} (q + q^i - q^j - q^k) \\ q_2 j &= \frac{1}{4} (q - q^i + q^j - q^k), & q_3 k &= \frac{1}{4} (q - q^i - q^j + q^k) \end{aligned}$$

of (3) which can be obtained by multiplying with  $\{1, i, j, k\}$  respectively. Furthermore, we can safely assume  $\frac{\partial \mathcal{L}}{\partial a^i} = \rho^i$ ,

$\frac{\partial \mathcal{L}}{\partial a^j} = p^j$  and  $\frac{\partial \mathcal{L}}{\partial a^k} = p^k$  due to Equations (21) and following (22). As required for the chain rule, we can further obtain

$$\begin{aligned}\frac{\partial \mathcal{L}}{\partial \delta_i^i} &= (p \circ \sigma'(\delta))^i \\ \frac{\partial \mathcal{L}}{\partial \delta_i^j} &= (p \circ \sigma'(\delta))^k \\ \frac{\partial \mathcal{L}}{\partial \delta_i^k} &= (p \circ \sigma'(\delta))^k\end{aligned}$$

following the same strategy.

2) *Derivative with respect to the weights:* Now we can continue with deriving the loss function with respect to the weights of a hidden layer.

**Theorem 5.** *The derivative of  $\mathcal{L}$  with respect to the weights of a hidden layer  $w_{i,j}^{(l)}$  of a QNN yields*

$$\frac{\partial \mathcal{L}(w)}{\partial w^{*(l)}} = q^* a^*$$

whereby  $q$  is the derivative of  $\mathcal{L}$  with respect to the following activation function.

*Proof.* For the derivative with respect to the hidden layers weights  $w_{i,j}^{(l)}$ , we need to calculate

$$\frac{\partial \mathcal{L}(\delta^{(l)}(w^{(l)}))}{\partial w^{*(l)}} = \frac{\partial \mathcal{L}}{\partial \delta} \frac{\partial \delta}{\partial w^*} + \frac{\partial \mathcal{L}}{\partial \delta^i} \frac{\partial \delta^i}{\partial w^*} + \frac{\partial \mathcal{L}}{\partial \delta^j} \frac{\partial \delta^j}{\partial w^*} + \frac{\partial \mathcal{L}}{\partial \delta^k} \frac{\partial \delta^k}{\partial w^*}.$$

Just like in the case above, we assign the name  $\frac{\partial \mathcal{L}}{\partial \delta^{(l)}} = q$  for the result. Then, we get the following partial derivatives for the involutions:

$$\frac{\partial y}{\partial \delta^i} = q^i, \quad \frac{\partial y}{\partial \delta^j} = q^j, \quad \frac{\partial y}{\partial \delta^k} = q^k$$

The right partial derivatives with respect to the weights are already known from Equations (15) and (16) in Subsection IV-B, namely

$$\frac{\partial \delta}{\partial w^*} = -\frac{1}{2} a^*, \quad \frac{\partial \delta^i}{\partial w^*} = \frac{1}{2} a^*, \quad \frac{\partial \delta^j}{\partial w^*} = \frac{1}{2} a^*, \quad \frac{\partial \delta^k}{\partial w^*} = \frac{1}{2} a^*$$

whereby  $\delta = \delta_i^{(l)}$ ,  $w = w_{i,j}^{(l)}$  and  $a = a_i^{(l-1)}$ . Consequently, the full derivation is

$$\begin{aligned}\frac{\partial \mathcal{L}(w)}{\partial w^*} &= \frac{\partial \mathcal{L}(\delta(w))}{\partial w^*} = q \frac{-1}{2} a^* + q^i \frac{1}{2} a^* + q^j \frac{1}{2} a^* + q^k \frac{1}{2} a^* \\ &= \frac{1}{2} (-q + q^i + q^j + q^k) a^* \stackrel{(5)}{=} q^* a^*\end{aligned}$$

which concludes the proof.  $\square$

3) *Derivative with respect to the biases:* Likewise, we need the derivative of the loss function with respect to the biases of a hidden layer

**Theorem 6.** *The derivative of  $\mathcal{L}$  with respect to the bias of a hidden layer  $b_i^{(l)}$  of a QNN yields*

$$\frac{\partial \mathcal{L}(b)}{\partial b^{*(l)}} = q^*$$

whereby  $q$  is the derivative of  $\mathcal{L}$  with respect to the following activation function.

*Proof.* In the same manner, we can also compute the derivation with respect to the bias  $b_i^{(l)}$

$$\frac{\partial \mathcal{L}(\delta^{(l)}(b^{(l)}))}{\partial b^{*(l)}} = \frac{\partial \mathcal{L}}{\partial \delta} \frac{\partial \delta}{\partial b^*} + \frac{\partial \mathcal{L}}{\partial \delta^i} \frac{\partial \delta^i}{\partial b^*} + \frac{\partial \mathcal{L}}{\partial \delta^j} \frac{\partial \delta^j}{\partial b^*} + \frac{\partial \mathcal{L}}{\partial \delta^k} \frac{\partial \delta^k}{\partial b^*}.$$

Using the known results

$$\frac{\partial \delta}{\partial b^*} = -\frac{1}{2}, \quad \frac{\partial \delta^i}{\partial b^*} = \frac{1}{2}, \quad \frac{\partial \delta^j}{\partial b^*} = \frac{1}{2}, \quad \frac{\partial \delta^k}{\partial b^*} = \frac{1}{2}$$

from Equations (18) and (19) the combined derivative yields

$$\begin{aligned}\frac{\partial \mathcal{L}(b)}{\partial b^*} &= \frac{\partial \mathcal{L}(\delta(b))}{\partial b^*} = q \frac{-1}{2} + q^i \frac{1}{2} + q^j \frac{1}{2} + q^k \frac{1}{2} \\ &= \frac{1}{2} (-q + q^i + q^j + q^k) \stackrel{(5)}{=} q^*.\end{aligned}$$

which concludes the proof.  $\square$

4) *Derivative with respect to the activations of the previous layer:* Finally, we need to derive with respect to the activation of the previous layer  $a_j^{(l-1)}$ . Again, the right partial derivatives are already known from Equation (20). As in the regular backpropagation, in this case we need to consider all neurons  $K$  where a respective activation  $a_j^{(l-1)}$  is input to.

**Theorem 7.** *The derivative of a hidden layer of a QNN with respect to its inputs, the activations  $a_j^{(l-1)}$  of a previous layer, is*

$$\frac{\partial \mathcal{L}(a_j^{(l-1)})}{\partial a_j^{(l-1)}} = \sum_{i \in K} q_i w_{i,j}$$

whereby  $q$  is the derivative of  $\mathcal{L}$  with respect to the following activation function

*Proof.* Just as in Theorem 3 we have to take the sum of the respective derivatives:

$$\begin{aligned}\frac{\partial \mathcal{L}(a_j^{(l-1)})}{\partial a_j^{(l-1)}} &= \sum_{i \in K} \frac{\partial \mathcal{L}(\delta_i^{(l)}(a_j^{(l-1)}))}{\partial a_j^{(l-1)}} \\ &= \sum_{i \in K} \frac{\partial \mathcal{L}}{\partial \delta_i} \frac{\partial \delta_i}{\partial a_j} + \frac{\partial \mathcal{L}}{\partial \delta_i^i} \frac{\partial \delta_i^i}{\partial a_j} + \frac{\partial \mathcal{L}}{\partial \delta_i^j} \frac{\partial \delta_i^j}{\partial a_j} + \frac{\partial \mathcal{L}}{\partial \delta_i^k} \frac{\partial \delta_i^k}{\partial a_j}\end{aligned}$$

By using the known derivatives from Equation (20) we obtain the final derivation

$$\frac{\partial \mathcal{L}(a_j^{(l-1)})}{\partial a_j^{(l-1)}} = \sum_{i \in K} q_i w_{i,j}$$

which concludes the proof.  $\square$

Likewise, we can obtain

$$\begin{aligned}\frac{\partial \mathcal{L}(a_j)}{\partial a_j^i} &= \sum_{i \in K} (a_i w_{i,j})^i \\ \frac{\partial \mathcal{L}(a_j)}{\partial a_j^j} &= \sum_{i \in K} (q_i w_{i,j})^j \\ \frac{\partial \mathcal{L}(a_j)}{\partial a_j^k} &= \sum_{i \in K} (q_i w_{i,j})^k.\end{aligned}\tag{22}$$



Note that the superscripts  $\square^{i,j,k}$  indicate the quaternion involutions and the subscripts  $\square_{i,j}$  the indices within the neural network. This result for a hidden layer ( $l$ ) is then the starting point when calculating the derivatives for optimizing the previous layer ( $l-1$ ) (compare Theorem 4).

5) *Update rules for the hidden layer:* Using the derived results, we can formulate the update rules for the parameters in the hidden layers as

$$\begin{aligned}\omega_{i,j}^{(l)}(n+1) &= \omega_{i,j}^{(l)}(n) - \lambda \left( p_{0_i}^{(l+1)} \sigma'(z_{0_i}^{(l)}) + p_{1_i}^{(l+1)} \sigma'(z_{1_i}^{(l)}) i \right. \\ &\quad \left. + p_{2_i}^{(l+1)} \sigma'(z_{2_i}^{(l)}) j + p_{3_i}^{(l+1)} \sigma'(z_{3_i}^{(l)}) k \right) a_j^{*(l-1)} \\ &= \omega_{i,j}^{(l)}(n) - \lambda \left( p_i^{(l)} \circ \sigma'(\hat{z}_i^{(l)}) \right) a_j^{*(l-1)} \\ \delta_i^{(l)}(n+1) &= \delta_i^{(l)}(n) - \lambda \left( p_{0_i}^{(l+1)} \sigma'(z_{0_i}^{(l)}) + p_{1_i}^{(l+1)} \sigma'(z_{1_i}^{(l)}) i \right. \\ &\quad \left. + p_{2_i}^{(l+1)} \sigma'(z_{2_i}^{(l)}) j + p_{3_i}^{(l+1)} \sigma'(z_{3_i}^{(l)}) k \right) a_j^{*(l-1)} \\ &= \delta_i^{(l)}(n) - \lambda \left( p_i^{(l)} \circ \sigma'(\hat{z}_i^{(l)}) \right) a_j^{*(l-1)}.\end{aligned}$$

Furthermore, the new  $p_j^{(l)}$  becomes

$$\begin{aligned}p_j^{(l)} &= \sum_{i \in K} \left( p_{0_i}^{(l+1)} \sigma'(z_{0_i}^{(l)}) + p_{1_i}^{(l+1)} \sigma'(z_{1_i}^{(l)}) i \right. \\ &\quad \left. + p_{2_i}^{(l+1)} \sigma'(z_{2_i}^{(l)}) j + p_{3_i}^{(l+1)} \sigma'(z_{3_i}^{(l)}) k \right) \omega_{i,j}^{(l)} \\ &= \sum_{i \in K} \left( p_i^{(l+1)} \circ \sigma'(\hat{z}_i^{(l)}) \right) \omega_{i,j}^{(l)}.\end{aligned}$$

Thus, all required derivatives to optimize a QNN beginning with the last layer backward to the first layer are derived and the quaternion backpropagation is complete.

## V. QUATERNION BACKPROPAGATION AND AUTOMATIC DIFFERENTIATION

As shown by [56], current deep learning libraries can be used to implement hypercomplex neural networks when using elementwise activation functions, e.g. by utilizing the Kronecker product. These libraries usually make use of automatic differentiation, allowing to train the implemented hypercomplex models without the necessity to define the respective derivatives. Naturally, the question arises how the relation is between automatic differentiation derivatives and the GHR derivatives. Consequently, this subsection investigates if automatic differentiation can be used to implement and train QNN following the derived optimization. We specifically target the automatic differentiation in PyTorch [57], although similar considerations could be made for other packages. For details on the automatic differentiation in PyTorch, we refer to [58].

### A. The relation of the GHR chain rule and chain rule in automatic differentiation

We start by making a general statement about the chain rule in automatic differentiation:

**Theorem 8.** *Assume a function  $f(y(x))$  and the derivative  $\frac{\partial f}{\partial y}$  to be  $s = s_0 + s_1 i + s_2 j + s_3 k$ . Then the derivative when*

*applying the chain rule on the individual quaternion elements  $y_0, y_1, y_2$  and  $y_3$  is*

$$\frac{\partial f}{\partial x} = \left( s^* \frac{\partial y}{\partial x} + s^{i*} \frac{\partial y^i}{\partial x} + s^{j*} \frac{\partial y^j}{\partial x} + s^{k*} \frac{\partial y^k}{\partial x} \right)^*.$$

*Proof.* As all input elements can be involved in the calculation of the respective output elements  $y_0, y_1, y_2$  and  $y_3$ , when calculating the derivative with respect to  $x_0, x_1, x_2$  and  $x_3$  all output elements have to be linked with the derivative components  $s_0, s_1, s_2$  and  $s_3$  to apply the chain rule on a component level. Consequently, the derivative formulates as

$$\begin{aligned}\frac{\partial f}{\partial x} &= \frac{\partial f(y(x))}{\partial x} \\ &= s_0 \frac{\partial y_0}{\partial x_0} + s_1 \frac{\partial y_1}{\partial x_0} + s_2 \frac{\partial y_2}{\partial x_0} + s_3 \frac{\partial y_3}{\partial x_0} \\ &\quad + \left( s_0 \frac{\partial y_0}{\partial x_1} + s_1 \frac{\partial y_1}{\partial x_1} + s_2 \frac{\partial y_2}{\partial x_1} + s_3 \frac{\partial y_3}{\partial x_1} \right) i \\ &\quad + \left( s_0 \frac{\partial y_0}{\partial x_2} + s_1 \frac{\partial y_1}{\partial x_2} + s_2 \frac{\partial y_2}{\partial x_2} + s_3 \frac{\partial y_3}{\partial x_2} \right) j \\ &\quad + \left( s_0 \frac{\partial y_0}{\partial x_3} + s_1 \frac{\partial y_1}{\partial x_3} + s_2 \frac{\partial y_2}{\partial x_3} + s_3 \frac{\partial y_3}{\partial x_3} \right) k \\ &\stackrel{(4)}{=} \frac{1}{4} (s^* + s^{i*} + s^{j*} + s^{k*}) \left( \frac{\partial y_0}{\partial x_0} + \frac{\partial y_0}{\partial x_1} i + \frac{\partial y_0}{\partial x_2} j + \frac{\partial y_0}{\partial x_3} k \right) \\ &\quad + \frac{i}{4} (s^* + s^{i*} - s^{j*} - s^{k*}) \left( \frac{\partial y_1}{\partial x_0} + \frac{\partial y_1}{\partial x_1} i + \frac{\partial y_1}{\partial x_2} j + \frac{\partial y_1}{\partial x_3} k \right) \\ &\quad + \frac{j}{4} (s^* - s^{i*} + s^{j*} - s^{k*}) \left( \frac{\partial y_2}{\partial x_0} + \frac{\partial y_2}{\partial x_1} i + \frac{\partial y_2}{\partial x_2} j + \frac{\partial y_2}{\partial x_3} k \right) \\ &\quad + \frac{k}{4} (s^* - s^{i*} - s^{j*} + s^{k*}) \left( \frac{\partial y_3}{\partial x_0} + \frac{\partial y_3}{\partial x_1} i + \frac{\partial y_3}{\partial x_2} j + \frac{\partial y_3}{\partial x_3} k \right) \\ &= s^* \frac{1}{4} \left[ \left( \frac{\partial y_0}{\partial x_0} + \frac{\partial y_0}{\partial x_1} i + \frac{\partial y_0}{\partial x_2} j + \frac{\partial y_0}{\partial x_3} k \right) \right. \\ &\quad + i \left( \frac{\partial y_1}{\partial x_0} + \frac{\partial y_1}{\partial x_1} i + \frac{\partial y_1}{\partial x_2} j + \frac{\partial y_1}{\partial x_3} k \right) \\ &\quad + j \left( \frac{\partial y_2}{\partial x_0} + \frac{\partial y_2}{\partial x_1} i + \frac{\partial y_2}{\partial x_2} j + \frac{\partial y_2}{\partial x_3} k \right) \\ &\quad \left. + k \left( \frac{\partial y_3}{\partial x_0} + \frac{\partial y_3}{\partial x_1} i + \frac{\partial y_3}{\partial x_2} j + \frac{\partial y_3}{\partial x_3} k \right) \right] \\ &\quad + s^{i*} \frac{1}{4} \left[ \left( \frac{\partial y_0}{\partial x_0} + \frac{\partial y_0}{\partial x_1} i + \frac{\partial y_0}{\partial x_2} j + \frac{\partial y_0}{\partial x_3} k \right) \right. \\ &\quad + i \left( \frac{\partial y_1}{\partial x_0} + \frac{\partial y_1}{\partial x_1} i + \frac{\partial y_1}{\partial x_2} j + \frac{\partial y_1}{\partial x_3} k \right) \\ &\quad - j \left( \frac{\partial y_2}{\partial x_0} + \frac{\partial y_2}{\partial x_1} i + \frac{\partial y_2}{\partial x_2} j + \frac{\partial y_2}{\partial x_3} k \right) \\ &\quad \left. - k \left( \frac{\partial y_3}{\partial x_0} + \frac{\partial y_3}{\partial x_1} i + \frac{\partial y_3}{\partial x_2} j + \frac{\partial y_3}{\partial x_3} k \right) \right] \\ &\quad + s^{j*} \frac{1}{4} \left[ \left( \frac{\partial y_0}{\partial x_0} + \frac{\partial y_0}{\partial x_1} i + \frac{\partial y_0}{\partial x_2} j + \frac{\partial y_0}{\partial x_3} k \right) \right. \\ &\quad - i \left( \frac{\partial y_1}{\partial x_0} + \frac{\partial y_1}{\partial x_1} i + \frac{\partial y_1}{\partial x_2} j + \frac{\partial y_1}{\partial x_3} k \right) \\ &\quad + j \left( \frac{\partial y_2}{\partial x_0} + \frac{\partial y_2}{\partial x_1} i + \frac{\partial y_2}{\partial x_2} j + \frac{\partial y_2}{\partial x_3} k \right) \\ &\quad \left. + k \left( \frac{\partial y_3}{\partial x_0} + \frac{\partial y_3}{\partial x_1} i + \frac{\partial y_3}{\partial x_2} j + \frac{\partial y_3}{\partial x_3} k \right) \right] \\ &\quad + s^{k*} \frac{1}{4} \left[ \left( \frac{\partial y_0}{\partial x_0} + \frac{\partial y_0}{\partial x_1} i + \frac{\partial y_0}{\partial x_2} j + \frac{\partial y_0}{\partial x_3} k \right) \right. \\ &\quad - i \left( \frac{\partial y_1}{\partial x_0} + \frac{\partial y_1}{\partial x_1} i + \frac{\partial y_1}{\partial x_2} j + \frac{\partial y_1}{\partial x_3} k \right) \\ &\quad - j \left( \frac{\partial y_2}{\partial x_0} + \frac{\partial y_2}{\partial x_1} i + \frac{\partial y_2}{\partial x_2} j + \frac{\partial y_2}{\partial x_3} k \right) \\ &\quad \left. + k \left( \frac{\partial y_3}{\partial x_0} + \frac{\partial y_3}{\partial x_1} i + \frac{\partial y_3}{\partial x_2} j + \frac{\partial y_3}{\partial x_3} k \right) \right]\end{aligned}$$

$$\begin{aligned}
& -k \left( \frac{\partial y_3}{\partial x_0} + \frac{\partial y_3}{\partial x_1} i + \frac{\partial y_3}{\partial x_2} j + \frac{\partial y_3}{\partial x_3} k \right) \\
& + s^{k*} \frac{1}{4} \left[ \left( \frac{\partial y_0}{\partial x_0} + \frac{\partial y_0}{\partial x_1} i + \frac{\partial y_0}{\partial x_2} j + \frac{\partial y_0}{\partial x_3} k \right) \right. \\
& - i \left( \frac{\partial y_1}{\partial x_0} + \frac{\partial y_1}{\partial x_1} i + \frac{\partial y_1}{\partial x_2} j + \frac{\partial y_1}{\partial x_3} k \right) \\
& - j \left( \frac{\partial y_2}{\partial x_0} + \frac{\partial y_2}{\partial x_1} i + \frac{\partial y_2}{\partial x_2} j + \frac{\partial y_2}{\partial x_3} k \right) \\
& \left. + k \left( \frac{\partial y_3}{\partial x_0} + \frac{\partial y_3}{\partial x_1} i + \frac{\partial y_3}{\partial x_2} j + \frac{\partial y_3}{\partial x_3} k \right) \right] \\
& = s^* \frac{1}{4} \left[ \frac{\partial y}{\partial x_0} + \frac{\partial y}{\partial x_1} i + \frac{\partial y}{\partial x_2} j + \frac{\partial y}{\partial x_3} k \right] \\
& + s^{i*} \frac{1}{4} \left[ \frac{\partial y^i}{\partial x_0} + \frac{\partial y^i}{\partial x_1} i + \frac{\partial y^i}{\partial x_2} j + \frac{\partial y^i}{\partial x_3} k \right] \\
& + s^{j*} \frac{1}{4} \left[ \frac{\partial y^j}{\partial x_0} + \frac{\partial y^j}{\partial x_1} i + \frac{\partial y^j}{\partial x_2} j + \frac{\partial y^j}{\partial x_3} k \right] \\
& + s^{k*} \frac{1}{4} \left[ \frac{\partial y^k}{\partial x_0} + \frac{\partial y^k}{\partial x_1} i + \frac{\partial y^k}{\partial x_2} j + \frac{\partial y^k}{\partial x_3} k \right] \\
& = s^* \frac{\partial y}{\partial x^*} + s^{i*} \frac{\partial y^i}{\partial x^*} + s^{j*} \frac{\partial y^j}{\partial x^*} + s^{k*} \frac{\partial y^k}{\partial x^*}.
\end{aligned}$$

□

In addition to this Theorem, we can further establish the following useful Corollaries:

**Corollary 1.** For a real valued function  $f(y(x))$  and  $\mu, \nu \in \mathbb{H} = 1$  where  $\frac{\partial f}{\partial y} = q$ , the GHR chain rule

$$\frac{\partial f}{\partial x} = \frac{\partial f}{\partial y} \frac{\partial y}{\partial x} + \frac{\partial f}{\partial y^i} \frac{\partial y^i}{\partial x} + \frac{\partial f}{\partial y^j} \frac{\partial y^j}{\partial x} + \frac{\partial f}{\partial y^k} \frac{\partial y^k}{\partial x}$$

simplifies to

$$\frac{\partial f}{\partial x} = q \frac{\partial y}{\partial x} + q^i \frac{\partial y^i}{\partial x} + q^j \frac{\partial y^j}{\partial x} + q^k \frac{\partial y^k}{\partial x}.$$

*Proof.* The relation

$$\left( \frac{\partial f}{\partial q} \right)^\eta = \frac{\partial f^\eta}{\partial q^\eta}$$

holds  $\forall \eta \in \{i, j, k\}$  [23]. For a real valued  $f$ ,

$$f^i = f^j = f^k = -i f i = -j f j = -k f k = f$$

and the corollary follows. □

This simplification is used from now on.

**Corollary 2.** Consider the function  $f(y(x))$  with  $\frac{\partial f}{\partial y} = q$ ,  $\frac{\partial f}{\partial y^i} = q^i$ ,  $\frac{\partial f}{\partial y^j} = q^j$  and  $\frac{\partial f}{\partial y^k} = q^k$  where the derivative  $\frac{\partial f}{\partial x}$  following the chain rule of the GHR calculus is

$$\frac{\partial f}{\partial x} = q \frac{\partial y}{\partial x} + q^i \frac{\partial y^i}{\partial x} + q^j \frac{\partial y^j}{\partial x} + q^k \frac{\partial y^k}{\partial x}.$$

Then, when applying the chain rule on the quaternion components, the derivative in automatic differentiation (AD) is

$$\frac{\partial f}{\partial x_{AD}} = \left( \frac{\partial f}{\partial x_{GHR}} \right)^*$$

when

$$\frac{\partial f}{\partial y_{AD}} = \left( \frac{\partial f}{\partial y_{GHR}} \right)^*.$$

*Proof.* The proof directly follows from Theorem 8 when choosing  $s = q^*$  and applying (10). □

To put that Corollary in simple words, one can conclude that the output derivative when applying the chain rule in automatic differentiation is the conjugate of the GHR derivative, as long as the input derivative is also the conjugate.

**Corollary 3.** Consider the function  $f(y(x))$  with  $\frac{\partial f}{\partial y} = q$ ,  $\frac{\partial f}{\partial y^i} = q^i$ ,  $\frac{\partial f}{\partial y^j} = q^j$  and  $\frac{\partial f}{\partial y^k} = q^k$  where the derivative  $\frac{\partial f}{\partial x^*}$  following the chain rule of the GHR calculus is

$$\frac{\partial f}{\partial x^*} = q \frac{\partial y}{\partial x^*} + q^i \frac{\partial y^i}{\partial x^*} + q^j \frac{\partial y^j}{\partial x^*} + q^k \frac{\partial y^k}{\partial x^*}.$$

Then, the relation

$$\frac{\partial f}{\partial x_{AD}} = \frac{\partial f}{\partial x^*_{GHR}}$$

holds, when

$$\frac{\partial f}{\partial y_{AD}} = \left( \frac{\partial f}{\partial y_{GHR}} \right)^*.$$

*Proof.* The proof also directly follows from Theorem 8 when choosing  $s = q^*$ . □

From this, we can state that the derivatives for GHR and automatic differentiation are the same, when the variable deriving for in automatic differentiation is the conjugate of the one in GHR calculus and the derivative connected using the chain rule is also the conjugate. This is of particular interest as for the direction of steepest descent in the GHR calculus one needs to derive with respect to  $\mathcal{W}^*$  and  $\mathcal{b}^*$  [23], [48] but when deriving for the individual components, we derive for  $w_0, w_1, w_2, w_3, b_0, b_1, b_2$  and  $w_3$  respectively, and thus not the conjugate.

In the following, we will continue with deriving the loss function as well as the derivatives with respect to  $\omega_{i,j}, b_i$  and  $a_j$  for the automatic differentiation. Specifically, Corollary 2 will be used together with the derivative with respect to the loss function for the gradients flowing backward through the model, and Corollary 3 for the derivatives with respect to the parameters.

## B. Forward phase and Loss function

Following [56], the real valued emulation of a quaternion linear layer with  $n$  inputs and  $m$  outputs is calculated as

$$\begin{bmatrix} \mathbf{w}_{1,1} & \mathbf{w}_{1,2} & \cdots & \mathbf{w}_{1,n} \\ \mathbf{w}_{2,1} & \mathbf{w}_{2,2} & \cdots & \mathbf{w}_{2,n} \\ \vdots & \vdots & \ddots & \vdots \\ \mathbf{w}_{m,1} & \mathbf{w}_{m,2} & \cdots & \mathbf{w}_{m,n} \end{bmatrix} \begin{bmatrix} \mathbf{a}_1 \\ \mathbf{a}_2 \\ \vdots \\ \mathbf{a}_n \end{bmatrix} + \begin{bmatrix} \mathbf{b}_1 \\ \mathbf{b}_2 \\ \vdots \\ \mathbf{b}_m \end{bmatrix} = \begin{bmatrix} \mathbf{z}_1 \\ \mathbf{z}_2 \\ \vdots \\ \mathbf{z}_m \end{bmatrix}$$

where  $\mathbf{w}_{i,j}$  is the real valued matrix representation of the quaternion  $\omega_{i,j}$  and  $\mathbf{a}_j, \mathbf{b}_i, \mathbf{z}_i$  the respective vector representations of  $a_i, b_i$  and  $z_i$ .

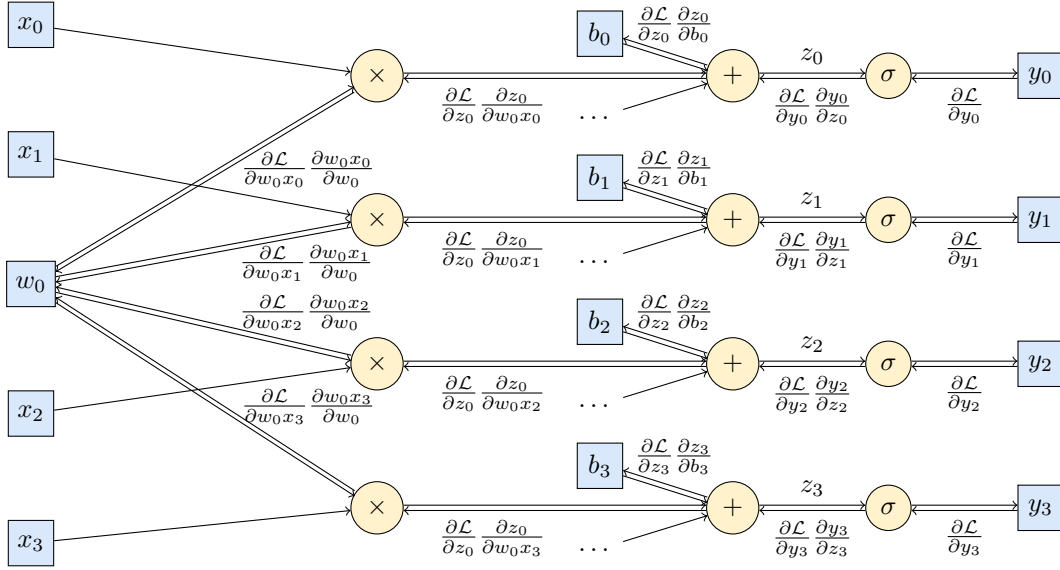


Fig. 1. Visualization of the gradient flow

Accordingly, one partial calculation is carried out as follows:

$$\mathbf{z}_i = \mathbf{w}_{i,j} \mathbf{a}_j + \mathbf{b}_i = \begin{bmatrix} w_0 & -w_1 & -w_2 & -w_3 \\ w_1 & w_0 & -w_3 & w_2 \\ w_2 & w_3 & w_0 & -w_1 \\ w_3 & -w_2 & w_1 & w_0 \end{bmatrix} \begin{bmatrix} a_0 \\ a_1 \\ a_2 \\ a_3 \end{bmatrix} + \begin{bmatrix} b_0 \\ b_1 \\ b_2 \\ b_3 \end{bmatrix}$$

The loss calculation as shown in Equation (12) remains unchanged.

Figure 1 further shows the information and gradient flow for an arbitrary hidden layer ( $l$ ). It is based on a visualization of a quaternion linear layer implementation in PyTorch [57] which we generated using PyTorchViz [59], shown in Figure 5 in Appendix D. For simplicity, we just show target  $w_0$  although the principle stays the same for remaining weights  $w_1$ ,  $w_2$  and  $w_3$ . For the final layer,  $\sigma$  is simply the identity function.

We again start by deriving the loss with respect to  $y_i$  and specifically to its components  $y_0, y_1, y_2$  and  $y_3$ . However, this time we do not compose them back in a quaternion but keep them as a vector, as the automatic differentiation does treat the outputs as completely independent of each other. Hence, we don't have derivatives as in Equations (7), (8) or (9). Instead, we get the simple derivatives

$$\begin{bmatrix} \frac{\partial \mathcal{L}}{\partial y_0} \\ \frac{\partial \mathcal{L}}{\partial y_1} \\ \frac{\partial \mathcal{L}}{\partial y_2} \\ \frac{\partial \mathcal{L}}{\partial y_3} \end{bmatrix} = -2 \begin{bmatrix} (d_0 - y_0) \\ (d_1 - y_1) \\ (d_2 - y_2) \\ (d_3 - y_3) \end{bmatrix} = -2 \begin{bmatrix} e_0 \\ e_1 \\ e_2 \\ e_3 \end{bmatrix} \quad (23)$$

which is the vector representation of  $-2e_i$ . We can observe that the derivative with respect to the models output  $y_i$  is the conjugate of the derivative obtained with the GHR calculus and greater by a factor of 4.

Note that in the calculations above we omitted the superscript  $\square^{(L)}$  indicating the layer and the subscripts  $\square_{i,j}$  indicating the row and column for better readability and to

avoid confusion with the subscript indicating the quaternion component. This is also what we are going to do in the following whenever possible.

### C. Derivative with respect to the inputs of the activation functions

When considering elementwise activation functions  $a^{(l)} = \sigma(z) = \sigma(z_0) + \sigma(z_1)i + \sigma(z_2)j + \sigma(z_3)k$ , the derivatives in automatic differentiation are straight forward

$$\begin{bmatrix} \frac{\partial a_0}{\partial z_0} \\ \frac{\partial a_1}{\partial z_1} \\ \frac{\partial a_2}{\partial z_2} \\ \frac{\partial a_3}{\partial z_3} \end{bmatrix} = \begin{bmatrix} \frac{\partial}{\partial z_0} \sigma(z_0) \\ \frac{\partial}{\partial z_1} \sigma(z_1) \\ \frac{\partial}{\partial z_2} \sigma(z_2) \\ \frac{\partial}{\partial z_3} \sigma(z_3) \end{bmatrix} = \begin{bmatrix} \sigma'(z_0) \\ \sigma'(z_1) \\ \sigma'(z_2) \\ \sigma'(z_3) \end{bmatrix}.$$

Thus, as in Theorem 4, the derivatives with respect to the activations are an elementwise multiplication with the derivative coming from the following layer ( $l+1$ ) during the backward phase. They don't change anything in terms of conjugation and scaling.

### D. Derivative with respect to the activation output of the previous layer

**Proposition 3.** Assume the derivative  $\frac{\partial \mathcal{L}}{\partial z}$  with respect to the output  $z^{(l)}$  of a quaternion linear layer ( $l$ ) to be  $q^* = q_0 - q_1i - q_2j - q_3k$ . Then, the derivative with respect to its input  $a_j^{(l-1)}$  in automatic differentiation is

$$\frac{\partial \mathcal{L} \left( a_j^{(l-1)} \right)}{\partial a_j^{(l-1)}} = \sum_{i \in K} (q_i w_{i,j})^*$$

and hence the conjugate as for the GHR derivatives with  $\frac{\partial \mathcal{L}}{\partial z} = q = q_0 + q_1i + q_2j + q_3k$ .

*Proof.* The proof follows directly from Theorem 7 and Corollary 2.  $\square$

Based on this, and the fact that an elementwise activation does not change anything in terms of conjugation, we can conclude that the gradient flow backwards through the whole model is the conjugate of the GHR gradients as long as the derivative with respect to the loss-function in automatic differentiation is the conjugate of the GHR derivative. From Equation (23) we know that this is the case. Furthermore, this result has the consequence that the gradient is also bigger by a factor of four. The detailed calculations are further shown in the Appendix E-A.

#### E. Derivative with respect to the weights

**Proposition 4.** Assume the derivative  $\frac{\partial \mathcal{L}}{\partial s}$  with respect to the output  $\tilde{z}_i^{(l)}$  of a quaternion linear layer ( $l$ ) to be  $q^* = q_0 - q_1i - q_2j - q_3k$ . Then, the derivative with respect to its weights  $\omega_{i,j}^{(l)}$  in automatic differentiation is

$$\frac{\partial \mathcal{L}(w)}{\partial \omega^{(l)}} = q^* a^*$$

and hence the same as for the GHR derivatives with  $\frac{\partial \mathcal{L}}{\partial s} = q = q_0 + q_1i + q_2j + q_3k$ .

*Proof.* The proof directly follows from Theorem 5 and Corollary 3.  $\square$

For the detailed calculations, compare with Appendix E-B. If we now insert the results from Equation (23), we obtain

$$\frac{\partial \mathcal{L}(w)}{\partial \omega^{(l)}} = -2ea^*.$$

As we can see, the weight updates for the final layer are four times as big as in the GHR Calculus (compare Theorem 1). This also holds for arbitrary hidden layers due to Proposition 3.

#### F. Derivative with respect to the bias

**Proposition 5.** Assume the derivative  $\frac{\partial \mathcal{L}}{\partial s}$  with respect to the output  $\tilde{z}_1^{(l)}$  of a quaternion linear layer ( $l$ ) to be  $q^* = q_0 - q_1i - q_2j - q_3k$ . Then, the derivative with respect to its bias  $b_i^{(l)}$  in automatic differentiation is

$$\frac{\partial \mathcal{L}(b)}{\partial b^{(l)}} = q^*$$

and hence the same as for the GHR derivatives with  $\frac{\partial \mathcal{L}}{\partial s} = q = q_0 + q_1i + q_2j + q_3k$ .

*Proof.* The proof directly follows from Theorem 6 and Corollary 3.  $\square$

Again, the detailed calculations are shown in Appendix E-C. Also here, if we insert the results from Equation (23), we obtain

$$\frac{\partial \mathcal{L}(b)}{\partial b^{(l)}} = -2e$$

and thus four times the derivative of Theorem 2. Likewise, gradients four times as big as the GHR gradients holds for the hidden layers due to Proposition 3.

## G. Implications

As we have shown, emulating QNN utilizing matrix-vector calculations in  $\mathbb{R}^4$  and elementwise activation functions as well as using automatic differentiation yields proper parameter updates according to the derived quaternion backpropagation. This can also be understood such that one has to apply the chain rule on the quaternion components instead of the whole quaternion when not using the GHR calculus. The user just has to be aware of two facts: the derivative with respect to the loss in automatic differentiation needs to be real valued and the conjugate of the GHR derivative and it can introduce a factor in the gradients, hence a learning rate correction might be desired, and the gradient flowing backwards through the model, the gradient with respect to the activations of the previous layers, is the conjugate of the GHR derivatives. Hence, one can benefit from the advantages of automatic differentiation as long as the limitations are known. Due to Theorem 8, arbitrary functions can be introduced in the model as long as the gradient flowing backwards through the model is the conjugate of the GHR gradient. Especially the usage of non elementwise operating activation functions within QNN is of particular interest here and something we aim to investigate in future work.

## VI. QUATERNIONIC TIME-SERIES COMPRESSION

Having introduced the required theoretical fundamentals, namely the quaternion backpropagation required to optimize QNN by means of gradient descent, we now proceed to describe the quaternionic time-series compression methodology where an overview is depicted in Figure 2.

The sensor readings are processed using the compression algorithm which we describe in more detail in the following subsection. This yields a shorter, quaternion valued time-series which is then fed into the QNN architecture

As a feature extractor, we use Dropout - Conv1d - Activation - Pooling blocks, followed by a flatten operation and Dropout - Linear - Activation blocks as a classifier. All of these layers are quaternion valued which will be described in more detail later. The final layer, however, is a conventional linear layer as there is no natural way to express a probability distribution or calculate a cross-entropy in quaternion space. Hence, it serves the purpose of a learnable mapping back from  $\mathbb{H} \rightarrow \mathbb{R}$ .

For comparison with real valued NNs, we create an equivalent by replacing all quaternion valued layers with real valued ones. As these are lacking the capability to deal with the quaternionic input data, we convert the input data of shape  $\mathbb{H}^{m \times k}$  into  $\mathbb{R}^{4m \times k}$ , i.e. for each quaternion channel of length  $k$  we create 4 channels of length  $k$ , carrying the information about min, max, mean and std. Consequently, that yields the relation of one quaternionic channel to four real valued ones.

### A. Compression Algorithm

As an attempt to shrink time-series data, an intuitive and often used approach is to downsample the data, e.g. by using the mean of the considered data segment. However, while doing so, there is an inherent information loss. For example, the mean does not reflect if there was large deviation in the

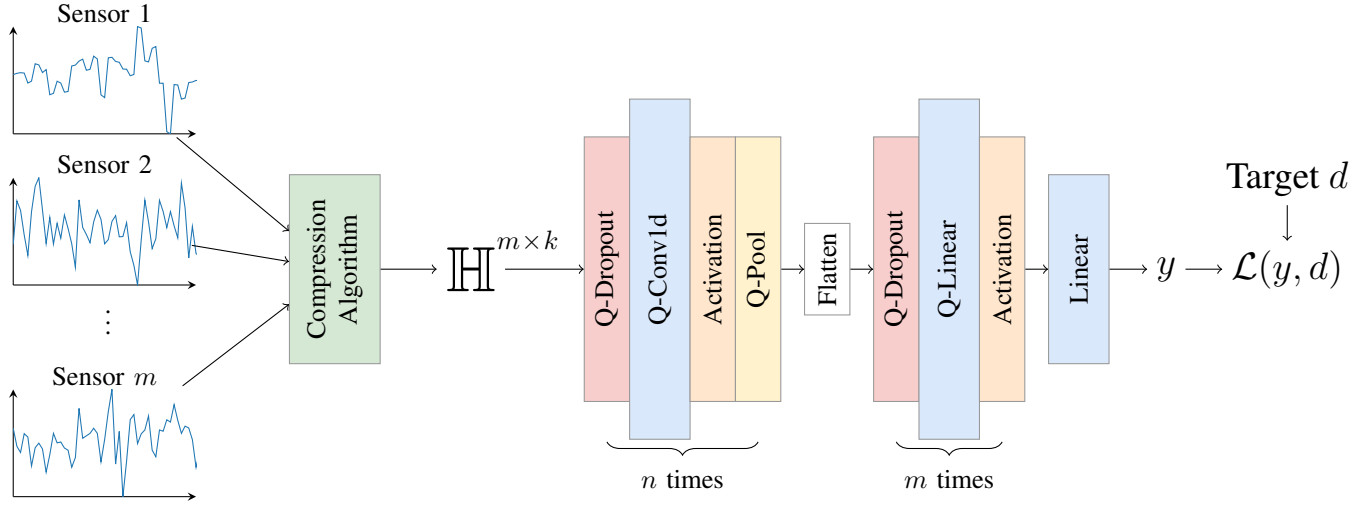


Fig. 2. Illustration of the quaternionic time-series compression methodology.

underlying data or if all values were relatively close to each other. To overcome this issue, multiple characteristics instead of just one can be used in an attempt to lower the information loss and create more representative, compressed data. As these statistics are related to each other, we propose to compose and gather them in a quaternion, specifically in the real and three imaginary parts. Hence, we obtain a mathematical object carrying the compressed information. Naturally, this yields a limit of four statistical values, for extensions one might consider octonion [60] or dual-quaternion [61], [62] based architectures. We will elaborate more on this in future work. In this study, we chose the min, max, mean and standard deviation for the descriptive properties as they are very intuitive in terms of representativeness and easy to obtain. Furthermore, this combination has showed good results in [63].

Assume a multivariate time-series consisting of  $m$  channels and  $n$  samples. Then, for all channels  $m$ , we divide the  $n$  samples into  $k$  parts of equal length  $l$ . In case  $n$  is not divisible by  $l$  without remainder, then the last chunk is of a shorter length. Subsequently, for all chunks, we determine the minimum, maximum, mean and standard deviation, which we store in the four components of a quaternion. Hence, we create a mapping from  $\mathbb{R}^{m \times n}$  into  $\mathbb{H}^{m \times k}$  whereby the compression rate is determined by the ratio  $l/4$ . The whole process is further illustrated by Figure 3.

		Chunk 1	Chunk 2	...	Chunk k
Sensor 1	$\mathbb{R}$	3 5 -1 7 4 9	3 1 -2 -2 0 5	...	7 3 2 1 2 6
	$\mathbb{H}$	-1.00	-2.00	...	1.00
		+9.00i	+5.00i	...	+7.00i
		+4.50j	+0.83j	...	+3.67j
		+3.45k	+2.79k	...	+2.42k
Sensor 2	$\mathbb{R}$	0 -1 2 4 3 6	1 0 -4 3 1 -1	...	0 -1 -3 -5 -4 -1
	$\mathbb{H}$	-1.00	-4.00	...	-5.00
		+6.00i	+3.00i	...	+0.00i
		+2.33j	+0.00j	...	-2.33j
		+2.58k	+2.37k	...	+1.97k

Fig. 3. Example illustrating the compression algorithm.

By employing the Hamilton product throughout the NN architecture, we ensure that the four features are used in a contiguous manner and emphasize the combined nature as well as their interrelationship within the proposed compression representation

### B. Quaternion valued Layer

In addition to the already described quaternion linear layer, for our model we use the following quaternion valued layers:

1) *1D Quaternion Convolution Layer*: To extract features from a quaternionic time-series, analog to the real valued equivalent, a one-dimensional convolution in quaternion space is required. Note that these layer can also be seen as a special case of the quaternion linear layer when treating the convolution as a matrix multiplication by a toeplitz matrix. For a quaternion valued input of size  $(B, C_{in}, L_{in})$  where  $B$  is the batch size,  $C_{in}$  are the input channels and  $L_{in}$  is the length of the multivariate input sequence, the  $i^{th}$  element of the output channel  $j$  using a kernel size  $K$  is calculated applying

$$y_{j,i} = b_j + \sum_{c=0}^{C_{in}-1} \sum_{k=0}^{K-1} x_{c,i+k} \otimes w_{j,c,k}$$

whereby the overall shape of the output is  $(B, C_{out}, L_{out})$ . Here, the weights are of size  $\mathbb{H}^{C_{out}, C_{in}, K}$  and the bias is of size  $\mathbb{H}^{C_{out}}$ . For ease of notation, we omit the dilation and the stride.

2) *Activations*: We employ element-wise working activation functions as proposed in [6], [15], [16]. Assuming an already known and tested activation  $\psi(\cdot)$  like ReLU or Tanh, the application on a quaternion input is

$$\psi(q) = \psi(q_0) + \psi(q_1)i + \psi(q_2)j + \psi(q_3)k.$$

The design and usage of activation functions specifically designed for the quaternion space provides an interesting direction for future research.

3) *1D Quaternion Max-Pooling*: Maximum-Pooling in quaternion space directly raises the question "What actually is the maximum of a set of multiple quaternions?" which has no distinct answer. This is due to the fact that it is composed out of four elements which can have their individual maximums, however they still have a combined meaning. In [64], an approach is proposed based on the amplitude or magnitude of a quaternion: it is used to construct a guidance matrix which selects the pooled quaternions based on the maximum magnitude out of a quaternion valued matrix. Contrary, [6] opts to consider and pool the real and three imaginary parts separately. In the following, we will describe both approaches in detail, as they tackle the problem from different views: the 1D Component Max-Pooling puts more emphasis on the individual maximums whereas the 1D Magnitude Max-Pooling emphasizes the combined relation of a quaternion.

a) *1D Quaternion Component Max-Pooling*: This approach considers the real part  $q_0$  and the imaginary parts  $q_1$ ,  $q_2$  and  $q_3$  separately. Specifically, using a kernel size  $K$ , the output is composed of the maximum of the  $K$  individual real parts and the respective  $K$  individual imaginary parts  $i$ ,  $j$  and  $k$ . This is described using

$$\begin{aligned} out(B_i, C_j, k) = & \\ & \max_{m=0, \dots, kernel\_size-1} \Re(in(N_i, C_j, stride \times k + m)) \\ + & \max_{m=0, \dots, kernel\_size-1} \Im(in(N_i, C_j, stride \times k + m))i \\ + & \max_{m=0, \dots, kernel\_size-1} \Im(in(N_i, C_j, stride \times k + m))j \\ + & \max_{m=0, \dots, kernel\_size-1} \Re(in(N_i, C_j, stride \times k + m))k. \end{aligned}$$

b) *1D Quaternion Magnitude Max-Pooling*: Contrary to the component-wise approach, here we consider the quaternion as a whole and use its norm  $\|q\|$  as a comparison measurement. Then, out of  $K$  considered quaternions, the one with the greatest norm is selected as the pooling output. We can formulate this process as

$$\begin{aligned} out(B_i, C_j, k) = in(N_i, C_j, l) \text{ where} \\ l = \underset{m=0, \dots, kernel\_size-1}{\operatorname{argmax}} in(N_i, C_j, \|stride \times k + m\|). \end{aligned}$$

As the norm operation is not affected by the sign of the quaternion components, using this approach it is more likely that negative values remain after pooling in comparison to the component max-pooling approach.

## VII. EXPERIMENTS

This section provides the experimental evaluation of the proposed methodology. We start with a regular supervised training including a test of the robustness against random parameter initialization. This is intended to prove the effectiveness of the proposed compression and to provide detailed comparison of quaternion valued with real valued architectures. This is followed by using the proposed approach in a self-supervised learning setup to highlight state-of-the-art performance. Finally, a detailed comparison with the literature is provided.

### A. Experimental setup

For our experimental evaluation, we use the TE dataset which consists of 21 fault cases and a regular operation case. In total, 52 variables are considered. For the training split, 480 samples are collected for the fault cases and 500 for the regular operation case. For the testing split, 960 samples are collected, whereby the fault was introduced after eight hours or 160 samples. We just consider the last 800 samples after the introduction of the fault in this work. Furthermore, we apply a sliding window of length 320 on the data. For our compression algorithm, we chose 40 chunks of length eight, yielding a compression-rate of factor two. Hence, we obtain data in the shape  $(N, 52, 4, 40)$  and  $(N, 208, 40)$ .

To incorporate different architectural choices, we use a combination of one convolution block with three linear blocks, two convolution blocks with four linear blocks and three convolution blocks with four linear blocks from which we design a narrow variant with a low amount of trainable parameters and a wide variant with a high amount of trainable parameters each. For the quaternion models, we use both presented pooling methods: the component pooling and the magnitude pooling to compare them in different learning setups. For the real valued comparison models, we also opt for two versions: The first is a model with an equal amount of trainable parameters, the second is a version which creates the same number of features as the layer outputs. However, this comes with the effect of having approximately four times the trainable parameters in the non-quaternion variant in comparison to the quaternion version. Furthermore, we add two baseline models to showcase the effect of the proposed compression: one for the uncompressed input and one using just a simple mean-resampling. Both utilize the same config as the real model with equal parameters, however due to the different input shape, the first convolution layer and consequently the first linear layer after the flatten operation is different. Hence, we end up with a total of 36 different model architectures to compare for our experiments. A detailed overview of the model configurations can be found in Table I.

For each model, we run a tuning with 50 trials from which 20 are warmup trials using the Python package Optuna [65] to obtain an optimized set of hyperparameters. Specifically, we tune for the following:

- Activation: ReLU, Tanh, Tanhshrink
- Learning Rate:  $1 \times 10^{-6}$  -  $1 \times 10^{-1}$
- Batch-size:  $2^4$  -  $2^8$
- Dropout ratio: 0, 0.1, 0.2, 0.3, 0.4

### B. Supervised Learning

In the fully supervised learning experiments, we trained 36 models in total. All of them were trained using the cross-entropy loss for 50 epochs each. This yielded the results provided in Table II.

As we can see, in all cases, the quaternion model outperformed its real valued counterparts. This is the case even when being in a disadvantage parameter-wise when comparing with the real eq. features model configuration. Thus, we can conclude that the quaternionic compression in combination

TABLE I  
USED NEURAL NETWORK CONFIGURATIONS

			params	conv output channel			linear output sizes			
1c3l	low	quat	327030	32			128	8	22	
		real equal params	327535	25x4			133	30	22	
		real equal feature space	1303926	32x4			512	32	22	
	high	quat	1859702	96			256	8	22	
		real equal params	1859146	85x4			256	32	22	
		real equal feature space	7432310	96x4			1024	32	22	
2c4l	low	quat	229366	32	32	32	128	128	8	22
		real equal params	229342	25x4	25x4	25x4	128	96	32	22
		real equal feature space	911350	32x4	32x4	32x4	512	512	32	22
	high	quat	1189366	96	96	96	256	256	8	22
		real equal params	1189749	73x4	73x4	73x4	259	256	32	22
		real equal feature space	4746742	96x4	96x4	96x4	1024	1024	32	22
3c4l	low	quat	163958	32	32	32	128	128	8	22
		real equal params	164998	23x4	22x4	22x4	96	60	24	22
		real equal feature space	649334	32x4	32x4	32x4	512	512	32	22
	high	quat	845686	96	96	96	256	256	8	22
		real equal params	853118	66x4	66x4	66x4	124	60	24	22
		real equal feature space	3370870	96x4	96x4	96x4	1024	1024	32	22

TABLE II  
ACCURACIES IN % OBTAINED USING THE SUPERVISED LEARNING SETUP.  
MAXIMUM VALUES ARE HIGHLIGHTED BOLD.

		quat		real		baseline	
		comp. pooling	mag. pooling	equal params	equal features	uncompressed	mean
1c3l	low	68.97	<b>70.82</b>	69.85	66.57	66.71	55.46
	high	68.58	<b>71.59</b>	66.95	68.59	70.07	52.39
2c4l	low	<b>71.16</b>	70.41	69.54	68.69	61.77	59.71
	high	<b>71.41</b>	68.90	67.08	69.72	60.94	52.66
3c4l	low	<b>69.87</b>	69.03	67.42	66.96	57.82	56.49
	high	69.70	<b>69.98</b>	66.90	68.99	53.13	56.82

with the quaternion valued model architecture outperforms the real valued counterparts being fed the same data in these experiments. In terms of quaternion pooling, no tendency is observable at this point as both versions achieved the respective highest accuracy three times. With the one exception of the 1c3l high configuration for the uncompressed baseline, in all baseline runs a significant drop in performance is existent. This highlights the advantages of compressing a long time-series for a fault classification task as proposed.

To investigate the effect of random initialization on the respective architectures, for each model we take the best set of hyperparameter, obtained from the experiments above, and train it again for 50 times using this specific set of hyperparameter. This yields the mean accuracies reported in Table III and maximum accuracies reported in Table IV. Furthermore, the accuracy distribution is shown in Figure 4.

It can be observed that one of the quaternion variants achieves the highest overall accuracies over all layer and parameter configurations, whereby the results are five to one in favor of the quaternion magnitude pooling. Similar outcomes can be identified in terms of the mean performance as four times the quaternion magnitude pooling performed best, one time the quaternion component pooling and one time the real

valued model with equal parameter count. Except for the 1c3l low configuration, both quaternion architectures obtained a higher mean and median accuracy than their real valued counterparts. Additionally, the quaternion variants show the tendency to have smaller variation and confidence intervals. Hence, especially with a limited budget on training runs, they are more likely to produce higher accuracies.

This overall highlights the advantage of using the quaternion valued models in this scenario. Furthermore, the magnitude pooling seems to be favorable in this fully supervised training setup, which we explain with its more regularizing behavior in comparison to the component pooling.

### C. Self-Supervised Learning

To further test state-of-the-art performance, we use the contrastive learning approach SimCLR-TS proposed by [66] which established a new baseline on the TE dataset. To prove the superiority of quaternion valued architectures in the proposed application, we replicate the contrastive learning setup and transfer it to our use case. For detailed information on SimCLR-TS, we refer to the original work.

We change the models in such a way that we only use the convolutional blocks with a flatten operation at the end for the contrastive learning. The following linear evaluation is done with a single linear layer, similar to SimCLR-TS. The tuning setup remains the same, however we add a second learning rate as SimCLR-TS is a two-staged methodology where a shared learning rate does not necessary make sense. The contrastive learning part is again trained for 50 epochs, for the following linear evaluation however it is sufficient to use 20 training epochs. Furthermore, in this experiment we use the two model configurations which obtained the highest accuracies in the supervised learning setup, namely 2c4l high and 3c4l low, with which we could obtain the results displayed in Table V.

As we can see, again the quaternion valued models outperform the real valued counterpart. The real-valued models

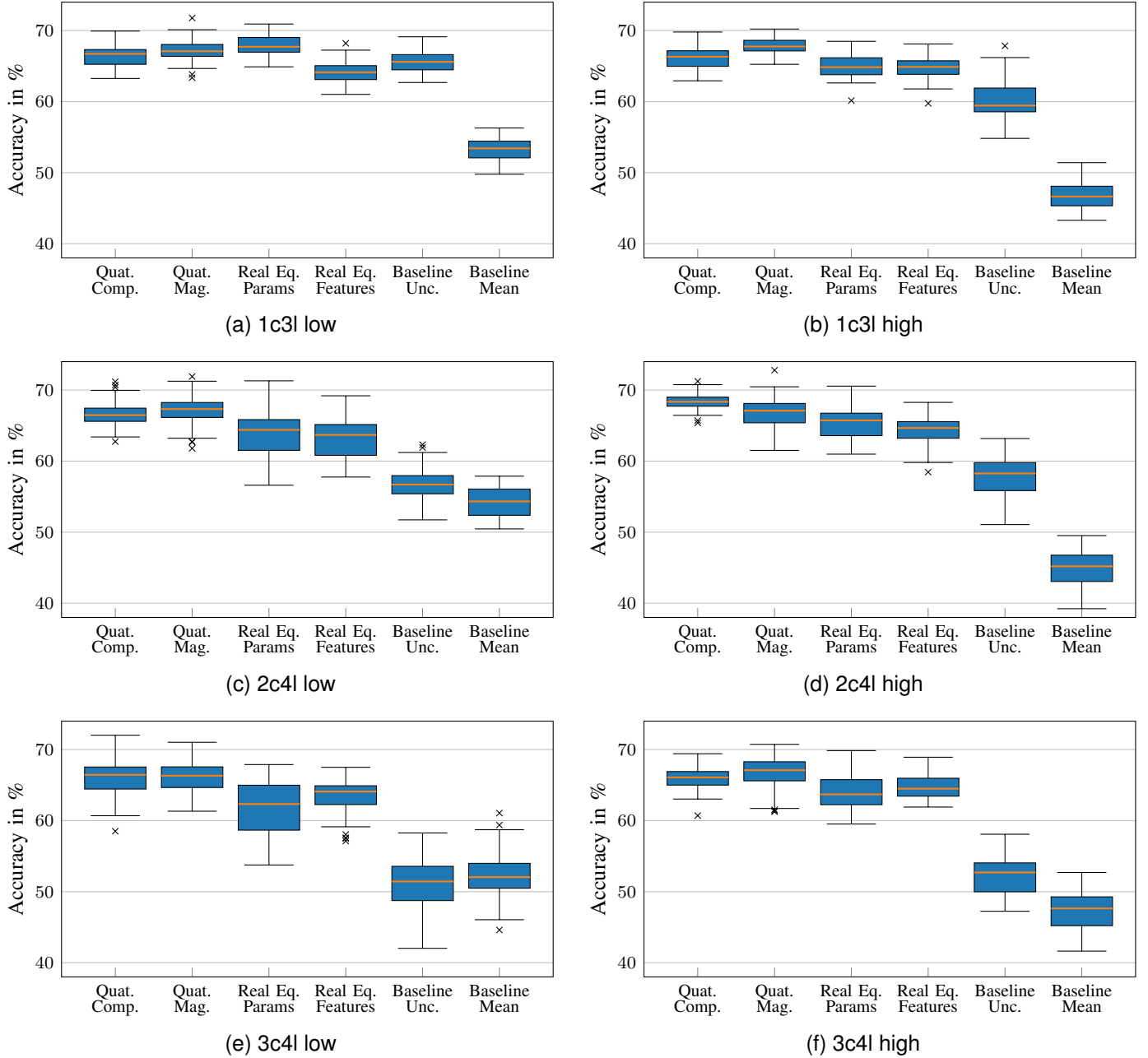


Fig. 4. Obtained results when training for 50 times with the best determined hyperparameter and different random parameter initialization. Note that in (f) one outlier at 4.55% for the real eq. features boxplot is not displayed.

benefit from the higher number of trainable parameters, but still remain inferior. Hence, also in a more advanced, state-of-the-art training setup, the usage of the Hamilton product within the convolutions allows for performance benefits and enables models with fewer trainable parameters. In these experiments, the component pooling outperformed the magnitude pooling. We attribute that to the fact that most of the training work is done in the self-supervised part, where the more regularizing effect of the magnitude pooling is not as beneficial as in a fully supervised training setup. Instead, the model performance benefits from the higher degree of flexibility offered by the component pooling.

#### D. Literature comparison

The TE dataset is widely used in machine learning research, however it also bears some problems in terms of comparability: Not always all of the 21 fault cases are used, and also sometimes not all sensor channels are used, hurting the comparability. Further, also varying windowing approaches are used to create the samples for training and testing. Finally, different evaluation metrics exist. Nevertheless, we want to compare our results with other works to put our proposed approach into context. Therefore, we provide a detailed set of results, obtained using a variety of approaches, in Table VI.

The first work using all fault cases we want to compare with



TABLE III

MEAN ACCURACIES IN % INCLUDING THE 95% CONFIDENCE INTERVAL OBTAINED IN THE RANDOM INITIALIZATION TEST. MAXIMUM VALUES ARE HIGHLIGHTED BOLD.

		quat		real		baseline	
		comp. pooling	mag. pooling	equal params	equal features	uncompressed	mean
1c3l	low	66.57 ± 3.09	67.20 ± 3.13	<b>67.92</b> ± 3.15	64.16 ± 3.13	65.69 ± 3.29	53.28 ± 3.23
	high	66.16 ± 3.19	<b>67.91</b> ± 2.42	65.00 ± 3.23	64.79 ± 3.43	60.31 ± 5.94	46.85 ± 3.98
2c4l	low	66.61 ± 3.48	<b>67.03</b> ± 4.39	63.90 ± 6.15	63.27 ± 5.93	56.81 ± 4.80	54.28 ± 4.28
	high	<b>68.34</b> ± 2.35	66.88 ± 4.14	65.53 ± 4.31	64.44 ± 4.18	57.97 ± 6.08	45.15 ± 5.29
3c4l	low	66.14 ± 5.19	<b>66.26</b> ± 4.11	61.87 ± 7.26	63.51 ± 5.09	51.35 ± 6.43	52.37 ± 6.50
	high	65.98 ± 3.46	<b>66.72</b> ± 4.60	63.96 ± 4.84	62.51 ± 24.25	52.45 ± 5.96	47.43 ± 4.95

TABLE IV

MAX ACCURACIES IN % OBTAINED IN THE RANDOM INITIALIZATION TEST. MAXIMUM VALUES ARE HIGHLIGHTED BOLD.

		quat		real		baseline	
		comp. pooling	mag. pooling	equal params	equal features	uncompressed	mean
1c3l	low	69.93	<b>71.77</b>	70.92	68.21	69.13	56.28
	high	69.80	<b>70.21</b>	68.48	68.12	67.85	51.41
2c4l	low	71.18	<b>71.91</b>	71.30	69.19	62.31	57.88
	high	71.23	<b>72.79</b>	70.55	68.27	63.17	49.52
3c4l	low	<b>72.02</b>	71.03	67.89	67.50	58.26	61.06
	high	69.41	<b>70.73</b>	69.85	68.92	58.08	52.69

TABLE V

ACCURACIES IN % OBTAINED USING THE SELF-SUPERVISED LEARNING SETUP. MAXIMUM VALUES ARE HIGHLIGHTED BOLD.

		quat		real		baseline	
		comp. pooling	mag. pooling	equal params	equal features	uncompressed	mean
2c4l	high	<b>83.90</b>	78.26	75.69	78.79	75.92	73.47
3c4l	low	<b>78.38</b>	76.52	76.25	77.51	72.57	65.68

is [67] where Support Vector Machines (SVM) and Principal Component Analysis (PCA) is used for fault classification on the TE dataset. Another relevant work that uses all error cases is [66] from which we adapted the semi-supervised learning. All of them, we could outperform with our best accuracy of 83.9% obtained using the 2c4l high configuration. Compared to SimCLR-TS, the biggest performance gains could be achieved on the difficult cases 3, 9 and 15 at the cost of performance losses in cases 0, 13 and 18.

Further, [68] employed stacked supervised auto-encoder, however they left out the most difficult cases 3, 9 15 which is a practice not untypical on TE. Since SimCLR-TS also reported a result for that setup, we likewise performed a training on this reduced cases setup. This yielded an accuracy of 93.58%, which is on par with SSAE. In almost all fault cases improvements over SimCLR-TS could be achieved, the only two exceptions are the regular operation case 0 with a slight drop of about 0.03%, the fault case 13 with a drop of 45,51% and case 16 with a drop of 0,61%, preventing an even bigger improvement.

In addition, there are other configurations using just a subset of the 22 cases of TE. In [70], Cases 16 - 21 as well as

the regular operation case were omitted when applying a random forest model. [69] proposes a multiscale convolutional neural network and long short-term memory (MCNN-LSTM), however they only apply it on cases 0, 1, 2, 4, 8, 10, 12, 13, 14, 17 and 18 of the TE-Process. Similarly, there is [71] which proposes a multichannel one-dimensional convolutional neural network (MC1-DCNN), however they omit the regular operation case 0 and also incorporate features from the frequency domain whereas we only work with compressed data in the time domain.

In contrast to leaving out fault cases, [72] leaves out sensor channels and only utilizes 33 channels of the dataset when doing process monitoring based on unstable neuron outputs in deep belief networks, and hence lacks comparability. Finally, [73] utilizes a CNN-pooling based architecture, however they do binary classification instead of having one model for all cases. Even though they report F1-scores instead of accuracies, we can state that our multi-class model is able to outperform the multiple binary ones.

## VIII. CONCLUSION

In this paper, we proposed a novel time-series compression approach for time-series data where we encode the minimum, maximum, mean and standard deviation of time-series extracts in a quaternion, yielding a quaternion valued time-series. Through the usage of the Hamilton product as the fundamental multiplication within QNNs, we were able to link these features in the quaternion convolution layer. Further, we developed a novel quaternion backpropagation utilizing the GHR-Calculus. After introducing the required fundamentals and quaternion mathematics, we showed that by using plain partial derivatives with respect to the quaternion components as in other approaches to quaternion backpropagation, the product and more critical, the chain rule, does not hold. By applying the GHR calculus, we end up with derivatives which do, to create our novel quaternion backpropagation algorithm. We further provided insights on the relation of automatic differentiation and quaternion backpropagation, and pointed out a scenario where automatic differentiation can be used to train QNN.

In the conducted experiments, quaternion valued models were able to outperform real valued counterparts in a fully supervised learning setup, utilizing the same compressed data, and also a baseline without any compression and a simple

TABLE VI

COMPARISON OF THE ACHIEVED ACCURACIES USING CONTRASTIVE LEARNING AND THE PROPOSED COMPRESSION METHOD WITH OTHER APPROACHES

Case	All cases				Without 3, 9, 15			other				
	SVM [67]	PCA [67]	SimCLR-TS [66]	2c4l high	SSAE [68]	SimCLR-TS [66]	2c4l high	MCNN-LSTM [69]	Enhanced RF [70]	MC1-DCNN [71]	UN-DBN [72] ‡	CNN [73] †
Case 0	19.27	19.69	<b>55.12</b>	37.42	96.48	<b>98.37</b>	98.34	93.5	-	-	-	-
Case 1	88.44	88.54	96.29	<b>100.0</b>	<b>100.0</b>	99.43	<b>100.0</b>	99.9	99	100.0	1	0.9139
Case 2	86.04	89.06	<b>100.0</b>	<b>100.0</b>	<b>100.0</b>	99.86	<b>100.0</b>	99.3	98	100.0	0.99	0.8796
Case 3	15.73	21.25	25.57	<b>73.18</b>	-	-	-	-	35	83.48	0.08	0.5059
Case 4	58.02	81.35	96.57	<b>100.0</b>	<b>100.0</b>	87.71	<b>100.0</b>	100	97	99.22	1	0.9973
Case 5	64.79	87.81	83.86	<b>100.0</b>	<b>100.0</b>	79.71	<b>100.0</b>	-	100	90.40	1	0.9035
Case 6	71.88	89.58	99.14	<b>100.0</b>	<b>100.0</b>	98.86	<b>100.0</b>	-	100	93.10	1	0.9150
Case 7	88.13	88.75	<b>100.0</b>	<b>100.0</b>	<b>100.0</b>	<b>100.0</b>	<b>100.0</b>	-	100	100.0	1	0.9155
Case 8	45.10	83.96	86.71	<b>96.47</b>	96.32	95.29	<b>100.0</b>	98.8	76	99.27	0.98	0.8295
Case 9	12.92	22.60	29.43	<b>53.85</b>	-	-	-	-	23	74.60	0.02	0.4953
Case 10	27.08	76.98	91.71	<b>100.0</b>	62.16	97.14	<b>98.54</b>	99.9	81	93.75	0.84	0.7005
Case 11	14.90	70.21	99.29	<b>100.0</b>	95.93	98.57	<b>100.0</b>	-	76	95.45	0.91	0.6016
Case 12	52.40	87.08	95.14	<b>100.0</b>	99.87	<b>100.0</b>	<b>100.0</b>	97.0	89	100.0	1	0.8666
Case 13	35.10	<b>69.58</b>	57.86	32.02	<b>89.88</b>	71.29	25.78	98.2	30	99.14	0.95	0.4692
Case 14	62.19	88.23	99.57	<b>100.0</b>	<b>100.0</b>	<b>100.0</b>	<b>100.0</b>	100	100	100.0	1	0.8868
Case 15	22.19	<b>26.98</b>	02.71	19.13	-	-	-	-	28	73.50	0.16	0.4354
Case 16	16.77	73.65	98.57	<b>98.96</b>	54.66	<b>99.57</b>	98.96	-	-	100.0	0.68	0.6684
Case 17	53.65	75.94	<b>100.0</b>	<b>100.0</b>	<b>100.0</b>	99.86	<b>100.0</b>	100	-	100.0	0.98	0.7711
Case 18	30.94	73.54	<b>99.00</b>	64.24	<b>93.56</b>	47.29	56.34	99.7	-	98.43	0.89	0.8274
Case 19	51.25	85.73	<b>100.0</b>	<b>100.0</b>	79.37	99.57	<b>100.0</b>	-	-	100.0	0.98	0.7087
Case 20	44.90	79.69	99.14	<b>100.0</b>	92.51	<b>100.0</b>	<b>100.0</b>	-	-	94.12	0.86	0.7288
Case 21	8.65	<b>85.63</b>	81.71	70.48	78.06	93.29	<b>100.0</b>	-	6	70.59	0.50	0.3126
<b>Overall</b>	44.11*	71.17*	81.43	<b>83.90</b>	91.52	93.00	<b>93.58</b>	98.8*	71.46	94.08	80.10*	0.7301*

\* Self calculated since it is not stated in original work

‡ Here a Detection Rate (DR) is stated

† Here the F1-score is stated instead of the fault detection accuracy

mean-resampling baseline. In a random initialization test, we could further show that these results hold for 50 different random model initialization. Furthermore, the quaternion variants showed the tendency to have lower variation and smaller confidence intervals. Also, in a self-supervised learning setup based on SimCLR-TS we could prove the superiority of the quaternion valued architectures, even outperforming the results from SimCLR-TS. Simultaneously, we compared two quaternion max-pooling variants, where the magnitude pooling showed an overall performance advantage in the fully supervised learning setup due to its more regularizing behavior, and the component pooling in the self supervised setup due to its higher degrees of flexibility.

Hence, we can conclude that quaternion valued architectures offer a performance advantage in this compression methodology over their real valued counterparts throughout all used model configurations and training setups.

In future work, we plan to investigate the impact or contribution of the individual properties used to form the quaternion for the final classification result. Based on these outcomes, other features representing the time-series extracts shall be observed to find the ideal combination of four properties. Also, we aim to investigate activation functions specifically tailored for quaternion models instead of using elementwise operating functions, with a particular focus on their derivatives and how the relation with automatic differentiation is in this scenario.

## REFERENCES

- [1] K. Cho, B. Van Merriënboer, D. Bahdanau, and Y. Bengio, "On the Properties of Neural Machine Translation: Encoder-Decoder Approaches," in *Proceedings of SSST-8, Eighth Workshop on Syntax, Semantics and Structure in Statistical Translation*. Doha, Qatar: Association for Computational Linguistics, 2014, pp. 103–111.
- [2] D. Bahdanau, K. Cho, and Y. Bengio, "Neural Machine Translation by Jointly Learning to Align and Translate," 2014, publisher: arXiv Version Number: 7.
- [3] L. B. Hinkle and V. Metsis, "Model Evaluation Approaches for Human Activity Recognition from Time-Series Data," in *Artificial Intelligence in Medicine*, A. Tucker, P. Henriques Abreu, J. Cardoso, P. Pereira Rodrigues, and D. Riaño, Eds. Cham: Springer International Publishing, 2021, vol. 12721, pp. 209–215, series Title: Lecture Notes in Computer Science.
- [4] S. Nakagome, T. P. Luu, Y. He, A. S. Ravindran, and J. L. Contreras-Vidal, "An empirical comparison of neural networks and machine learning algorithms for EEG gait decoding," *Scientific Reports*, vol. 10, no. 1, p. 4372, Mar. 2020.
- [5] E. Keogh, K. Chakrabarti, M. Pazzani, and S. Mehrotra, "Dimensionality Reduction for Fast Similarity Search in Large Time Series Databases," *Knowledge and Information Systems*, vol. 3, no. 3, pp. 263–286, Aug. 2001.
- [6] X. Zhu, Y. Xu, H. Xu, and C. Chen, "Quaternion Convolutional Neural Networks," in *Proceedings of the European Conference on Computer Vision (ECCV)*, Sep. 2018.
- [7] T. Parcollet, M. Morchid, and G. Linares, "Quaternion Convolutional Neural Networks for Heterogeneous Image Processing," in *ICASSP 2019 - 2019 IEEE International Conference on Acoustics, Speech and Signal Processing (ICASSP)*. Brighton, United Kingdom: IEEE, May 2019, pp. 8514–8518.
- [8] A. Hirose, Ed., *Complex-valued neural networks: advances and applications*, ser. IEEE Press series on computational intelligence. Hoboken, N.J: John Wiley & Sons Inc, 2013, oCLC: ocn812254892.
- [9] C. Trabelsi, O. Bilaniuk, Y. Zhang, D. Serdyuk, S. Subramanian, J. F. Santos, S. Mehri, N. Rostamzadeh, Y. Bengio, and C. J. Pal, "Deep Complex Networks," 2017, publisher: arXiv Version Number: 4.
- [10] N. Benvenuto and F. Piazza, "On the complex backpropagation algorithm," *IEEE Transactions on Signal Processing*, vol. 40, no. 4, pp. 967–969, Apr. 1992.
- [11] Y. Ishizuka, S. Murai, Y. Takahashi, M. Kawai, Y. Taniyai, and T. Naniwa, "Modeling Walking Behavior of Powered Exoskeleton Based

- on Complex-Valued Neural Network,” in *2018 IEEE International Conference on Systems, Man, and Cybernetics (SMC)*. Miyazaki, Japan: IEEE, Oct. 2018, pp. 1927–1932.
- [12] C.-A. Popa, “Complex-valued convolutional neural networks for real-valued image classification,” in *2017 International Joint Conference on Neural Networks (IJCNN)*. Anchorage, AK, USA: IEEE, May 2017, pp. 816–822.
- [13] D. Hayakawa, T. Masuko, and H. Fujimura, “Applying Complex-Valued Neural Networks to Acoustic Modeling for Speech Recognition,” in *2018 Asia-Pacific Signal and Information Processing Association Annual Summit and Conference (APSIPA ASC)*. Honolulu, HI, USA: IEEE, Nov. 2018, pp. 1725–1731.
- [14] W. Shen, B. Zhang, S. Huang, Z. Wei, and Q. Zhang, “3D-Rotation-Equivariant Quaternion Neural Networks,” in *Computer Vision – ECCV 2020*, A. Vedaldi, H. Bischof, T. Brox, and J.-M. Frahm, Eds. Cham: Springer International Publishing, 2020, vol. 12365, pp. 531–547, series Title: Lecture Notes in Computer Science.
- [15] T. Parcollet, M. Morchid, P.-M. Bousquet, R. Dufour, G. Linares, and R. De Mori, “Quaternion Neural Networks for Spoken Language Understanding,” in *2016 IEEE Spoken Language Technology Workshop (SLT)*. San Diego, CA: IEEE, Dec. 2016, pp. 362–368.
- [16] T. Parcollet, M. Ravanelli, M. Morchid, G. Linares, and R. De Mori, “Speech recognition with quaternion neural networks,” 2018, publisher: arXiv Version Number: 1.
- [17] C. J. Gaudet and A. S. Maida, “Deep Quaternion Networks,” in *2018 International Joint Conference on Neural Networks (IJCNN)*. Rio de Janeiro: IEEE, Jul. 2018, pp. 1–8.
- [18] U. Onyekpe, V. Palade, S. Kanarachos, and S.-R. Christopoulos, “A Quaternion Gated Recurrent Unit Neural Network for Sensor Fusion,” *Information*, vol. 12, no. 3, p. 117, Mar. 2021.
- [19] P. Arena, L. Fortuna, G. Muscato, and M. Xibilia, “Multilayer Perceptrons to Approximate Quaternion Valued Functions,” *Neural Networks*, vol. 10, no. 2, pp. 335–342, Mar. 1997.
- [20] T. Nitta, “A quaternary version of the back-propagation algorithm,” *Proceedings of ICNN’95 - International Conference on Neural Networks*, vol. 5, pp. 2753–2756, 1995.
- [21] T. Parcollet, M. Ravanelli, M. Morchid, G. Linares, C. Trabelsi, R. De Mori, and Y. Bengio, “Quaternion Recurrent Neural Networks,” 2018, publisher: arXiv Version Number: 3.
- [22] N. Matsui, T. Isokawa, H. Kusamichi, and F. Peper, “Quaternion Neural Network with Geometrical Operators,” *J. Intell. Fuzzy Syst.*, no. 15, pp. 149–164, 2004.
- [23] D. Xu, C. Jahanchahi, C. C. Took, and D. P. Mandic, “Enabling quaternion derivatives: the generalized HR calculus,” *Royal Society Open Science*, vol. 2, no. 8, p. 150255, Aug. 2015.
- [24] D. Xu, Y. Xia, and D. P. Mandic, “Optimization in Quaternion Dynamic Systems: Gradient, Hessian, and Learning Algorithms,” *IEEE transactions on neural networks and learning systems*, vol. 27, no. 2, pp. 249–261, Feb. 2016.
- [25] D. Blalock, S. Madden, and J. Gutttag, “Sprintz: Time Series Compression for the Internet of Things,” *Proceedings of the ACM on Interactive, Mobile, Wearable and Ubiquitous Technologies*, vol. 2, no. 3, pp. 1–23, Sep. 2018.
- [26] A. Gómez-Brandón, J. R. Paramá, K. Villalobos, A. Illarramendi, and N. R. Brisaboa, “Lossless compression of industrial time series with direct access,” *Computers in Industry*, vol. 132, p. 103503, Nov. 2021.
- [27] G. Campobello, A. Segreto, S. Zanafi, and S. Serrano, “RAKE: A simple and efficient lossless compression algorithm for the Internet of Things,” in *2017 25th European Signal Processing Conference (EUSIPCO)*. Kos, Greece: IEEE, Aug. 2017, pp. 2581–2585.
- [28] J. Spiegel, P. Wira, and G. Hermann, “A Comparative Experimental Study of Lossless Compression Algorithms for Enhancing Energy Efficiency in Smart Meters,” in *2018 IEEE 16th International Conference on Industrial Informatics (INDIN)*. Porto: IEEE, Jul. 2018, pp. 447–452.
- [29] H. S. Mogahed and A. G. Yakunin, “Development of a Lossless Data Compression Algorithm for Multichannel Environmental Monitoring Systems,” in *2018 XIV International Scientific-Technical Conference on Actual Problems of Electronics Instrument Engineering (APEIE)*. Novosibirsk: IEEE, Oct. 2018, pp. 483–486.
- [30] G. Luo, K. Yi, S.-W. Cheng, Z. Li, W. Fan, C. He, and Y. Mu, “Piecewise linear approximation of streaming time series data with maximum error guarantees,” in *2015 IEEE 31st International Conference on Data Engineering*. Seoul, South Korea: IEEE, Apr. 2015, pp. 173–184.
- [31] Yongwei Ding, Xiaohu Yang, A. J. Kavs, and Juefeng Li, “A novel piecewise linear segmentation for time series,” in *2010 The 2nd International Conference on Computer and Automation Engineering (ICCAE)*. Singapore: IEEE, Feb. 2010, pp. 52–55.
- [32] X. Kitsios, P. Liakos, K. Papakonstantinopoulou, and Y. Kotidis, “Simple-Piece: Highly Accurate Piecewise Linear Approximation through Similar Segment Merging,” *Proc. {VLDB} Endow.*, vol. 16, no. 8, pp. 1910–1922, 2023.
- [33] F. Eichinger, P. Efron, S. Karnouskos, and K. Böhm, “A time-series compression technique and its application to the smart grid,” *The VLDB Journal*, vol. 24, no. 2, pp. 193–218, Apr. 2015.
- [34] D. Lemire, “A Better Alternative to Piecewise Linear Time Series Segmentation,” in *Proceedings of the 2007 SIAM International Conference on Data Mining*. Society for Industrial and Applied Mathematics, Apr. 2007, pp. 545–550.
- [35] A. Ukil, S. Bandyopadhyay, and A. Pal, “IoT Data Compression: Sensor-Agnostic Approach,” in *2015 Data Compression Conference*. Snowbird, UT, USA: IEEE, Apr. 2015, pp. 303–312.
- [36] S. Di and F. Cappello, “Fast Error-Bounded Lossy HPC Data Compression with SZ,” in *2016 IEEE International Parallel and Distributed Processing Symposium (IPDPS)*. Chicago, IL, USA: IEEE, May 2016, pp. 730–739.
- [37] S. Chandak, K. Tatwawadi, C. Wen, L. Wang, J. Aparicio Ojea, and T. Weissman, “LFZip: Lossy Compression of Multivariate Floating-Point Time Series Data via Improved Prediction,” in *2020 Data Compression Conference (DCC)*. Snowbird, UT, USA: IEEE, Mar. 2020, pp. 342–351.
- [38] J. Azar, A. Makhoul, R. Couturier, and J. Demerjian, “Robust IoT time series classification with data compression and deep learning,” *Neurocomputing*, vol. 398, pp. 222–234, Jul. 2020.
- [39] O. P. Concha, R. Y. D. Xu, and M. Piccardi, “Compressive Sensing of Time Series for Human Action Recognition,” in *2010 International Conference on Digital Image Computing: Techniques and Applications*. Sydney, Australia: IEEE, Dec. 2010, pp. 454–461.
- [40] J. Azar, A. Makhoul, M. Barhamgi, and R. Couturier, “An energy efficient IoT data compression approach for edge machine learning,” *Future Generation Computer Systems*, vol. 96, pp. 168–175, Jul. 2019.
- [41] L. Karamitopoulos and G. Evangelidis, “A Dispersion-Based PAA Representation for Time Series,” in *2009 WRI World Congress on Computer Science and Information Engineering*. Los Angeles, California USA: IEEE, 2009, pp. 490–494.
- [42] B. Lkhagva, Yu Suzuki, and K. Kawagoe, “New Time Series Data Representation ESAX for Financial Applications,” in *22nd International Conference on Data Engineering Workshops (ICDEW’06)*. Atlanta, GA, USA: IEEE, 2006, pp. x115–x115.
- [43] D. E. Rumelhart, G. E. Hinton, and R. J. Williams, “Learning representations by back-propagating errors,” *Nature*, vol. 323, no. 6088, pp. 533–536, Oct. 1986.
- [44] H. Leung and S. Haykin, “The complex backpropagation algorithm,” *IEEE Transactions on Signal Processing*, vol. 39, no. 9, pp. 2101–2104, Sep. 1991.
- [45] T. Nitta, “An Extension of the Back-Propagation Algorithm to Complex Numbers,” *Neural Networks*, vol. 10, no. 8, pp. 1391–1415, Nov. 1997.
- [46] D. T. La Corte and Y. M. Zou, “Newton’s Method Backpropagation for Complex-Valued Holomorphic Multilayer Perceptrons,” 2014, publisher: arXiv Version Number: 1.
- [47] K. Kreutz-Delgado, “The Complex Gradient Operator and the CR-Calculus,” 2009, publisher: arXiv Version Number: 1.
- [48] D. P. Mandic, C. Jahanchahi, and C. C. Took, “A Quaternion Gradient Operator and Its Applications,” *IEEE Signal Processing Letters*, vol. 18, no. 1, pp. 47–50, Jan. 2011.
- [49] E. Grassucci, D. Comminiello, and A. Uncini, “A Quaternion-Valued Variational Autoencoder,” in *ICASSP 2021 - 2021 IEEE International Conference on Acoustics, Speech and Signal Processing (ICASSP)*. Toronto, ON, Canada: IEEE, Jun. 2021, pp. 3310–3314.
- [50] E. Grassucci, E. Cicero, and D. Comminiello, “Quaternion Generative Adversarial Networks,” in *Generative Adversarial Learning: Architectures and Applications*, R. Razavi-Far, A. Ruiz-Garcia, V. Palade, and J. Schmidhuber, Eds. Cham: Springer International Publishing, 2022, vol. 217, pp. 57–86, series Title: Intelligent Systems Reference Library.
- [51] A. Muppidi and M. Radfar, “Speech Emotion Recognition Using Quaternion Convolutional Neural Networks,” in *ICASSP 2021 - 2021 IEEE International Conference on Acoustics, Speech and Signal Processing (ICASSP)*. Toronto, ON, Canada: IEEE, Jun. 2021, pp. 6309–6313.
- [52] S. Qin, X. Zhang, H. Xu, and Y. Xu, “Fast Quaternion Product Units for Learning Disentangled Representations in  $\mathbb{SO}(3)$ ,” *IEEE Transactions on Pattern Analysis and Machine Intelligence*, pp. 1–17, 2022.
- [53] W. R. Hamilton, “II. On quaternions; or on a new system of imaginaries in algebra,” *The London, Edinburgh, and Dublin Philosophical Magazine and Journal of Science*, vol. 25, no. 163, pp. 10–13, Jul. 1844.

- [54] T. A. Ell and S. J. Sangwine, "Quaternion involutions and anti-involutions," *Computers & Mathematics with Applications*, vol. 53, no. 1, pp. 137–143, Jan. 2007.
- [55] A. Sudbery, "Quaternionic analysis," *Mathematical Proceedings of the Cambridge Philosophical Society*, vol. 85, no. 2, pp. 199–225, Mar. 1979.
- [56] M. E. Valle, "Understanding Vector-Valued Neural Networks and Their Relationship with Real and Hypercomplex-Valued Neural Networks," 2023, publisher: arXiv Version Number: 1.
- [57] A. Paszke, S. Gross, F. Massa, A. Lerer, J. Bradbury, G. Chanan, T. Killeen, Z. Lin, N. Gimelshein, L. Antiga, A. Desmaison, A. Köpf, E. Yang, Z. DeVito, M. Raison, A. Tejani, S. Chilamkurthy, B. Steiner, L. Fang, J. Bai, and S. Chintala, *PyTorch: an imperative style, high-performance deep learning library*. Red Hook, NY, USA: Curran Associates Inc., 2019.
- [58] A. Paszke, S. Gross, S. Chintala, G. Chanan, E. Yang, Z. DeVito, Z. Lin, A. Desmaison, L. Antiga, and A. Lerer, "Automatic differentiation in pytorch," in *NIPS-W*, 2017.
- [59] S. Zagoruyko, "Pytorchviz," <https://github.com/szagoruyko/pytorchviz>, 2021, v0.0.2.
- [60] C.-A. Popa, "Octonion-Valued Neural Networks," in *Artificial Neural Networks and Machine Learning – ICANN 2016*, A. E. Villa, P. Masulli, and A. J. Pons Rivero, Eds. Cham: Springer International Publishing, 2016, vol. 9886, pp. 435–443, series Title: Lecture Notes in Computer Science.
- [61] J. Pöppelbaum and A. Schwung, "Predicting Rigid Body Dynamics Using Dual Quaternion Recurrent Neural Networks With Quaternion Attention," *IEEE Access*, vol. 10, pp. 82 923–82 943, 2022.
- [62] A. Schwung, J. Pöppelbaum, and P. C. Nutakki, "Rigid Body Movement Prediction Using Dual Quaternion Recurrent Neural Networks," in *2021 22nd IEEE International Conference on Industrial Technology (ICIT)*. Valencia, Spain: IEEE, Mar. 2021, pp. 756–761.
- [63] C. Guo, M. Lu, and J. Chen, "An evaluation of time series summary statistics as features for clinical prediction tasks," *BMC Medical Informatics and Decision Making*, vol. 20, no. 1, p. 48, Dec. 2020.
- [64] Q. Yin, J. Wang, X. Luo, J. Zhai, S. K. Jha, and Y.-Q. Shi, "Quaternion Convolutional Neural Network for Color Image Classification and Forensics," *IEEE Access*, vol. 7, pp. 20 293–20 301, 2019.
- [65] T. Akiba, S. Sano, T. Yanase, T. Ohta, and M. Koyama, "Optuna: A Next-generation Hyperparameter Optimization Framework," in *Proceedings of the 25th ACM SIGKDD International Conference on Knowledge Discovery & Data Mining*. Anchorage AK USA: ACM, Jul. 2019, pp. 2623–2631.
- [66] J. Pöppelbaum, G. S. Chadha, and A. Schwung, "Contrastive learning based self-supervised time-series analysis," *Applied Soft Computing*, vol. 117, p. 108397, Mar. 2022.
- [67] C. Jing, X. Gao, X. Zhu, and S. Lang, "Fault classification on Tennessee Eastman process: PCA and SVM," in *2014 International Conference on Mechatronics and Control (ICMC)*. Jinzhou, China: IEEE, Jul. 2014, pp. 2194–2197.
- [68] Y. Wang, H. Yang, X. Yuan, Y. A. Shardt, C. Yang, and W. Gui, "Deep learning for fault-relevant feature extraction and fault classification with stacked supervised auto-encoder," *Journal of Process Control*, vol. 92, pp. 79–89, Aug. 2020.
- [69] J. Yuan and Y. Tian, "A Multiscale Feature Learning Scheme Based on Deep Learning for Industrial Process Monitoring and Fault Diagnosis," *IEEE Access*, vol. 7, pp. 151 189–151 202, 2019.
- [70] Z. Chai and C. Zhao, "Enhanced Random Forest With Concurrent Analysis of Static and Dynamic Nodes for Industrial Fault Classification," *IEEE Transactions on Industrial Informatics*, vol. 16, no. 1, pp. 54–66, Jan. 2020.
- [71] J. Yu, C. Zhang, and S. Wang, "Multichannel one-dimensional convolutional neural network-based feature learning for fault diagnosis of industrial processes," *Neural Computing and Applications*, vol. 33, no. 8, pp. 3085–3104, Apr. 2021.
- [72] J. Yu and X. Yan, "Whole Process Monitoring Based on Unstable Neuron Output Information in Hidden Layers of Deep Belief Network," *IEEE Transactions on Cybernetics*, vol. 50, no. 9, pp. 3998–4007, Sep. 2020.
- [73] G. Singh Chadha, M. Krishnamoorthy, and A. Schwung, "Time Series based Fault Detection in Industrial Processes using Convolutional Neural Networks," in *IECON 2019 - 45th Annual Conference of the IEEE Industrial Electronics Society*. Lisbon, Portugal: IEEE, Oct. 2019, pp. 173–178.

## APPENDIX A HR-CALCULUS

Similar to the CR-Calculus [47], [48] introduces the HR-Calculus as a method to derive quaternion valued functions. This enables deriving holomorphic quaternionic functions as well as nonholomorphic real functions of quaternion variables. The quaternion derivatives are derived as

$$\begin{aligned}\frac{\partial f}{\partial q} &= \frac{1}{4} \left( \frac{\partial f}{\partial q_0} - \frac{\partial f}{\partial q_1} i - \frac{\partial f}{\partial q_2} j - \frac{\partial f}{\partial q_3} k \right) \\ \frac{\partial f}{\partial q^i} &= \frac{1}{4} \left( \frac{\partial f}{\partial q_0} - \frac{\partial f}{\partial q_1} i + \frac{\partial f}{\partial q_2} j + \frac{\partial f}{\partial q_3} k \right) \\ \frac{\partial f}{\partial q^j} &= \frac{1}{4} \left( \frac{\partial f}{\partial q_0} + \frac{\partial f}{\partial q_1} i - \frac{\partial f}{\partial q_2} j + \frac{\partial f}{\partial q_3} k \right) \\ \frac{\partial f}{\partial q^k} &= \frac{1}{4} \left( \frac{\partial f}{\partial q_0} + \frac{\partial f}{\partial q_1} i + \frac{\partial f}{\partial q_2} j - \frac{\partial f}{\partial q_3} k \right).\end{aligned}\quad (24)$$

The corresponding conjugate derivatives are defined as

$$\begin{aligned}\frac{\partial f}{\partial q^*} &= \frac{1}{4} \left( \frac{\partial f}{\partial q_0} + \frac{\partial f}{\partial q_1} i + \frac{\partial f}{\partial q_2} j + \frac{\partial f}{\partial q_3} k \right) \\ \frac{\partial f}{\partial q^{i*}} &= \frac{1}{4} \left( \frac{\partial f}{\partial q_0} + \frac{\partial f}{\partial q_1} i - \frac{\partial f}{\partial q_2} j - \frac{\partial f}{\partial q_3} k \right) \\ \frac{\partial f}{\partial q^{j*}} &= \frac{1}{4} \left( \frac{\partial f}{\partial q_0} - \frac{\partial f}{\partial q_1} i + \frac{\partial f}{\partial q_2} j - \frac{\partial f}{\partial q_3} k \right) \\ \frac{\partial f}{\partial q^{k*}} &= \frac{1}{4} \left( \frac{\partial f}{\partial q_0} - \frac{\partial f}{\partial q_1} i - \frac{\partial f}{\partial q_2} j + \frac{\partial f}{\partial q_3} k \right).\end{aligned}$$

**Proposition 6.** *When deriving a quaternion valued function  $f(q)$ ,  $q \in \mathbb{H}$  using (24) and the known product rule from  $\mathbb{R}$ , the product rule also does not apply.*

*Proof.* Again consider  $f(q) = qq^* = q_0^2 + q_1^2 + q_2^2 + q_3^2$  as the function of choice. Then the direct derivation is

$$\begin{aligned}\frac{\partial f}{\partial q} &= \frac{1}{4} \left( \frac{\partial f}{\partial q_0} - \frac{\partial f}{\partial q_1} i - \frac{\partial f}{\partial q_2} j - \frac{\partial f}{\partial q_3} k \right) \\ &= \frac{1}{4} (2q_0 - 2q_1 i - 2q_2 j - 2q_3 k) \\ &= \frac{1}{2} q^*\end{aligned}$$

Using the product rule, we can calculate the same derivation using

$$\frac{\partial}{\partial q} qq^* = q \frac{\partial q^*}{\partial q} + \frac{\partial q}{\partial q} q^* \quad (25)$$

Calculating the partial results

$$\frac{\partial q^*}{\partial q} = \frac{1}{4} (1 + ii + jj + kk) = -\frac{1}{2}$$

and

$$\frac{\partial q}{\partial q} = \frac{1}{4} (1 - ii - jj - kk) = 1$$

and inserting back into (25) yields

$$\begin{aligned}\frac{\partial}{\partial q} qq^* &= q \frac{\partial q^*}{\partial q} + \frac{\partial q}{\partial q} q^* \\ &= -\frac{1}{2} q + 1q^* \neq \frac{1}{2} q^*\end{aligned}$$

□

APPENDIX B  
GHR-CALCULUS

**Example 1.** When using the GHR-Calculus and definitions, product rule can be used as follows:

*Solution:* Again consider  $f(q) = qq^* = q_0^2 + q_1^2 + q_2^2 + q_3^2$  as the function of choice. Then the direct derivation is

$$\begin{aligned}\frac{\partial f}{\partial q} &= \frac{1}{4} \left( \frac{\partial f}{\partial q_0} - \frac{\partial f}{\partial q_1} i - \frac{\partial f}{\partial q_2} j - \frac{\partial f}{\partial q_3} k \right) \\ &= \frac{1}{4} (2q_0 - 2q_1 i - 2q_2 j - 2q_3 k) \\ &= \frac{1}{2} q^*\end{aligned}$$

Using the product rule, we can calculate the same derivation using

$$\frac{\partial(qq^*)}{\partial q^\mu} = q \frac{\partial(q^*)}{\partial q^\mu} + \frac{\partial(q)}{\partial q^{\mu*}} q^* = q \frac{\partial(q^*)}{\partial q} + \frac{\partial(q)}{\partial q^{\mu*}} q^* \text{ with } \mu = 1 \quad (26)$$

Calculating the partial results

$$\frac{\partial(q^*)}{\partial q^\mu} = \frac{-1}{2} \quad (\text{same as for HR with } \mu = 1)$$

and

$$\begin{aligned}\frac{\partial(q)}{\partial q^{q^*}} &= \frac{1}{4} \left( \frac{\partial f}{\partial q_0} - \frac{\partial f}{\partial q_1} i^{q^*} - \frac{\partial f}{\partial q_2} j^{q^*} - \frac{\partial f}{\partial q_3} k^{q^*} \right) \\ &= \frac{1}{4} (1 - ii^{q^*} - jj^{q^*} - kk^{q^*}) \\ &= \frac{1}{4} (q^* q^{*-1} - iq^* i q^{*-1} - jq^* j q^{*-1} - kq^* k q^{*-1}) \\ &= \frac{1}{4} (q^* - iq^* i - jq^* j - kq^* k) q^{*-1} \\ &= \frac{1}{4} (q^* + q^{i*} + q^{j*} + q^{k*}) q^{*-1} \\ &= q_0 q^{*-1}\end{aligned}$$

and inserting back into (26) yields

$$\begin{aligned}\frac{\partial(qq^*)}{\partial q^\mu} &= q \frac{\partial(q^*)}{\partial q^\mu} + \frac{\partial(q)}{\partial q^{\mu*}} q^* \\ &= \frac{-1}{2} q + q_0 q^{*-1} q^* \\ &= \frac{-1}{2} (q_0 + q_1 i + q_2 j + q_3 k) + q_0 \\ &= \frac{1}{2} (q_0 - q_1 i - q_2 j - q_3 k) \\ &= \frac{1}{2} q^*.\end{aligned}$$

APPENDIX C  
DETAILED DERIVATIVE CALCULATIONS

A. Detailed calculations for the derivatives of  $\mathcal{L}$  with respect to the involutions  $y^i$ ,  $y^j$  and  $y^k$

$$\begin{aligned}\frac{\partial \mathcal{L}}{\partial y^i} &= \frac{\partial}{\partial y^i} [(d_0 - y_0)^2 + (d_1 - y_1)^2 + (d_2 - y_2)^2 + (d_3 - y_3)^2] \\ &= \frac{1}{4} [-2(d_0 - y_0) + 2(d_1 - y_1)i - 2(d_2 - y_2)j - 2(d_3 - y_3)k] \\ &= -\frac{1}{2} [(d_0 - y_0) - (d_1 - y_1)i + (d_2 - y_2)j + (d_3 - y_3)k] \\ &= -\frac{1}{2} (d - y)^{i*} = -\frac{1}{2} e^{i*}\end{aligned}$$

$$\begin{aligned}\frac{\partial \mathcal{L}}{\partial y^j} &= \frac{\partial}{\partial y^j} [(d_0 - y_0)^2 + (d_1 - y_1)^2 + (d_2 - y_2)^2 + (d_3 - y_3)^2] \\ &= \frac{1}{4} [-2(d_0 - y_0) - 2(d_1 - y_1)i + 2(d_2 - y_2)j - 2(d_3 - y_3)k] \\ &= -\frac{1}{2} [(d_0 - y_0) + (d_1 - y_1)i - (d_2 - y_2)j + (d_3 - y_3)k] \\ &= -\frac{1}{2} (d - y)^{j*} = -\frac{1}{2} e^{j*}\end{aligned}$$

$$\begin{aligned}\frac{\partial \mathcal{L}}{\partial y^k} &= \frac{\partial}{\partial y^k} [(d_0 - y_0)^2 + (d_1 - y_1)^2 + (d_2 - y_2)^2 + (d_3 - y_3)^2] \\ &= \frac{1}{4} [-2(d_0 - y_0) - 2(d_1 - y_1)i - 2(d_2 - y_2)j + 2(d_3 - y_3)k] \\ &= -\frac{1}{2} [(d_0 - y_0) + (d_1 - y_1)i + (d_2 - y_2)j - (d_3 - y_3)k] \\ &= -\frac{1}{2} (d - y)^{k*} = -\frac{1}{2} e^{k*}\end{aligned}$$

B. Detailed calculations for the derivatives of the involutions  $y^i$ ,  $y^j$  and  $y^k$  with respect to  $w^*$

$$\begin{aligned}\frac{\partial y^i}{\partial w^*} &= \frac{\partial(wa + b)^i}{\partial w^*} = \frac{\partial(wa)^i}{\partial w^*} \\ &= \frac{\partial}{\partial w^*} [(a_0 w_0 - a_1 w_1 - a_2 w_2 - a_3 w_3) \\ &\quad + (a_0 w_1 + a_1 w_0 - a_2 w_3 + a_3 w_2)i \\ &\quad - (a_0 w_2 + a_1 w_3 + a_2 w_0 - a_3 w_1)j \\ &\quad - (a_0 w_3 - a_1 w_2 + a_2 w_1 + a_3 w_0)k] \\ &= \frac{1}{4} [a_0 + a_1 i - a_2 j - a_3 k + (a_0 i - a_1 - a_2 k + a_3 j)i \\ &\quad + (-a_0 j + a_1 k - a_2 + a_3 i)j + (-a_0 k - a_1 j - a_2 i - a_3)k] \\ &= \frac{1}{2} [a_0 - a_1 i - a_2 j - a_3 k] \\ &= \frac{1}{2} a^*\end{aligned}$$

$$\begin{aligned}
\frac{\partial y^j}{\partial w^*} &= \frac{\partial(wa + b)^j}{\partial w^*} = \frac{\partial(wa)^j}{\partial w^*} \\
&= \frac{\partial}{\partial w^*} [(a_0w_0 - a_1w_1 - a_2w_2 - a_3w_3) \\
&\quad - (a_0w_1 + a_1w_0 - a_2w_3 + a_3w_2)i \\
&\quad + (a_0w_2 + a_1w_3 + a_2w_0 - a_3w_1)j \\
&\quad - (a_0w_3 - a_1w_2 + a_2w_1 + a_3w_0)k] \\
&= \frac{1}{4} [a_0 - a_1i + a_2j - a_3k + (-a_0i - a_1 - a_2k - a_3j)i \\
&\quad + (a_0j + a_1k - a_2 - a_3i)j + (-a_0k + a_1j + a_2i - a_3)k] \\
&= \frac{1}{2} [a_0 - a_1i - a_2j - a_3k] \\
&= \frac{1}{2} a^*
\end{aligned}$$

$$\begin{aligned}
\frac{\partial y^k}{\partial b^*} &= \frac{\partial(wa + b)^k}{\partial b^*} = \frac{\partial(b)^k}{\partial b^*} \\
&= \frac{\partial}{\partial b^*} (b_0 - b_1i - b_2j + b_3k) \\
&= \frac{1}{4} (1 - ii - jj + kk) \\
&= \frac{1}{4} (1 + 1 + 1 - 1) \\
&= 0.5
\end{aligned}$$

*D. Detailed calculations for the derivatives of  $y$ ,  $y^i$ ,  $y^j$  and  $y^k$  with respect to  $a$*

$$\begin{aligned}
\frac{\partial y^k}{\partial w^*} &= \frac{\partial(wa + b)^k}{\partial w^*} = \frac{\partial(wa)^k}{\partial w^*} \\
&= \frac{\partial}{\partial w^*} [(a_0w_0 - a_1w_1 - a_2w_2 - a_3w_3) \\
&\quad - (a_0w_1 + a_1w_0 - a_2w_3 + a_3w_2)i \\
&\quad - (a_0w_2 + a_1w_3 + a_2w_0 - a_3w_1)j \\
&\quad + (a_0w_3 - a_1w_2 + a_2w_1 + a_3w_0)k] \\
&= \frac{1}{4} [a_0 - a_1i - a_2j + a_3k + (-a_0i - a_1 + a_2k + a_3j)i \\
&\quad + (-a_0j - a_1k - a_2 - a_3i)j + (a_0k - a_1j + a_2i - a_3)k] \\
&= \frac{1}{2} [a_0 - a_1i - a_2j - a_3k] \\
&= \frac{1}{2} a^*
\end{aligned}$$

$$\begin{aligned}
\frac{\partial y}{\partial a} &= \frac{\partial(wa + b)}{\partial a} = \frac{\partial(wa)}{\partial a} \\
&= \frac{\partial}{\partial a} [(a_0w_0 - a_1w_1 - a_2w_2 - a_3w_3) \\
&\quad + (a_0w_1 + a_1w_0 - a_2w_3 + a_3w_2)i \\
&\quad + (a_0w_2 + a_1w_3 + a_2w_0 - a_3w_1)j \\
&\quad + (a_0w_3 - a_1w_2 + a_2w_1 + a_3w_0)k] \\
&= \frac{1}{4} [(w_0 + w_1i + w_2j + w_3k) - (w_0i - w_1 - w_2k + w_3j)i \\
&\quad - (w_0j + w_1k - w_2 - w_3i)j - (w_0k - w_1j + w_2i - w_3)k] \\
&= w_0 + w_1i + w_2j + w_3k \\
&= w
\end{aligned}$$

*C. Detailed calculations for the derivatives of the involutions  $y^i$ ,  $y^j$  and  $y^k$  with respect to  $b^*$*

$$\begin{aligned}
\frac{\partial y^i}{\partial b^*} &= \frac{\partial(wa + b)^i}{\partial b^*} = \frac{\partial(b)^i}{\partial b^*} \\
&= \frac{\partial}{\partial b^*} (b_0 + b_1i - b_2j - b_3k) \\
&= \frac{1}{4} (1 + ii - jj - kk) \\
&= \frac{1}{4} (1 - 1 + 1 + 1) \\
&= 0.5
\end{aligned}$$

$$\begin{aligned}
\frac{\partial y^j}{\partial b^*} &= \frac{\partial(wa + b)^j}{\partial b^*} = \frac{\partial(b)^j}{\partial b^*} \\
&= \frac{\partial}{\partial b^*} (b_0 - b_1i + b_2j - b_3k) \\
&= \frac{1}{4} (1 - ii + jj - kk) \\
&= \frac{1}{4} (1 + 1 - 1 + 1) \\
&= 0.5
\end{aligned}$$

$$\begin{aligned}
\frac{\partial y^i}{\partial a} &= \frac{\partial(wa + b)^i}{\partial a} = \frac{\partial(wa)^i}{\partial a} \\
&= \frac{\partial}{\partial a} [(a_0w_0 - a_1w_1 - a_2w_2 - a_3w_3) \\
&\quad + (a_0w_1 + a_1w_0 - a_2w_3 + a_3w_2)i \\
&\quad - (a_0w_2 + a_1w_3 + a_2w_0 - a_3w_1)j \\
&\quad - (a_0w_3 - a_1w_2 + a_2w_1 + a_3w_0)k] \\
&= \frac{1}{4} [(w_0 + w_1i - w_2j - w_3k) - (w_0i - w_1 + w_2k - w_3j)i \\
&\quad - (-w_0j - w_1k - w_2 - w_3i)j - (-w_0k + w_1j + w_2i - w_3)k] \\
&= 0
\end{aligned}$$

$$\begin{aligned}
\frac{\partial y^j}{\partial a} &= \frac{\partial(wa + b)^j}{\partial a} = \frac{\partial(wa)^j}{\partial a} \\
&= \frac{\partial}{\partial a} [(a_0w_0 - a_1w_1 - a_2w_2 - a_3w_3) \\
&\quad - (a_0w_1 + a_1w_0 - a_2w_3 + a_3w_2)i \\
&\quad + (a_0w_2 + a_1w_3 + a_2w_0 - a_3w_1)j \\
&\quad - (a_0w_3 - a_1w_2 + a_2w_1 + a_3w_0)k] \\
&= \frac{1}{4} [(w_0 - w_1i + w_2j - w_3k) - (-w_0i - w_1 + w_2k + w_3j)i \\
&\quad - (w_0j - w_1k - w_2 + w_3i)j - (-w_0k - w_1j - w_2i - w_3)k] \\
&= 0
\end{aligned}$$

$$\begin{aligned}
\frac{\partial y^k}{\partial a} &= \frac{\partial(wa + \beta)^k}{\partial a} = \frac{\partial(wa)^k}{\partial a} \\
&= \frac{\partial}{\partial a} [(a_0 w_0 - a_1 w_1 - a_2 w_2 - a_3 w_3) \\
&\quad - (a_0 w_1 + a_1 w_0 - a_2 w_3 + a_3 w_2) i \\
&\quad - (a_0 w_2 + a_1 w_3 + a_2 w_0 - a_3 w_1) j \\
&\quad + (a_0 w_3 - a_1 w_2 + a_2 w_1 + a_3 w_0) k] \\
&= \frac{1}{4} [(w_0 - w_1 i - w_2 j + w_3 k) - (-w_0 i - w_1 - w_2 k - w_3 j) i \\
&\quad - (-w_0 j + w_1 k - w_2 + w_3 i) j - (w_0 k + w_1 j - w_2 i - w_3) k] \\
&= 0
\end{aligned}$$

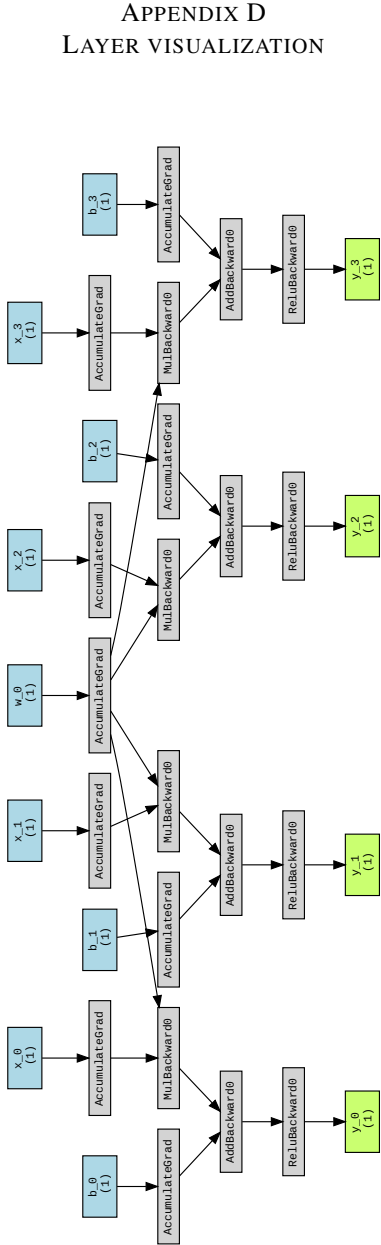


Fig. 5. Visualization of the gradient flow for parameter  $w_0$  obtained with TorchViz

## APPENDIX E

### AUTOMATIC DIFFERENTIATION CALCULATIONS

*A. Derivative with respect to the activation output of the previous layer*

The derivative with respect to the layers input  $a^{(l-1)}$  is calculated as

$$\begin{aligned}
\begin{bmatrix} \frac{\partial \mathcal{L}}{\partial a_0} \\ \frac{\partial \mathcal{L}}{\partial a_1} \\ \frac{\partial \mathcal{L}}{\partial a_2} \\ \frac{\partial \mathcal{L}}{\partial a_3} \end{bmatrix} &= \sum_{i \in K} \begin{bmatrix} \frac{\partial \mathcal{L}}{\partial z_{i0}} \frac{\partial z_{i0}}{\partial a_0} + \frac{\partial \mathcal{L}}{\partial z_{i1}} \frac{\partial z_{i1}}{\partial a_0} + \frac{\partial \mathcal{L}}{\partial z_{i2}} \frac{\partial z_{i2}}{\partial a_0} + \frac{\partial \mathcal{L}}{\partial z_{i3}} \frac{\partial z_{i3}}{\partial a_0} \\ \frac{\partial \mathcal{L}}{\partial z_{i0}} \frac{\partial z_{i0}}{\partial a_1} + \frac{\partial \mathcal{L}}{\partial z_{i1}} \frac{\partial z_{i1}}{\partial a_1} + \frac{\partial \mathcal{L}}{\partial z_{i2}} \frac{\partial z_{i2}}{\partial a_1} + \frac{\partial \mathcal{L}}{\partial z_{i3}} \frac{\partial z_{i3}}{\partial a_1} \\ \frac{\partial \mathcal{L}}{\partial z_{i0}} \frac{\partial z_{i0}}{\partial a_2} + \frac{\partial \mathcal{L}}{\partial z_{i1}} \frac{\partial z_{i1}}{\partial a_2} + \frac{\partial \mathcal{L}}{\partial z_{i2}} \frac{\partial z_{i2}}{\partial a_2} + \frac{\partial \mathcal{L}}{\partial z_{i3}} \frac{\partial z_{i3}}{\partial a_2} \\ \frac{\partial \mathcal{L}}{\partial z_{i0}} \frac{\partial z_{i0}}{\partial a_3} + \frac{\partial \mathcal{L}}{\partial z_{i1}} \frac{\partial z_{i1}}{\partial a_3} + \frac{\partial \mathcal{L}}{\partial z_{i2}} \frac{\partial z_{i2}}{\partial a_3} + \frac{\partial \mathcal{L}}{\partial z_{i3}} \frac{\partial z_{i3}}{\partial a_3} \end{bmatrix} \\
&= \sum_{i \in K} \begin{bmatrix} q_{i0} w_{i,j_0} - q_{i1} w_{i,j_1} - q_{i2} w_{i,j_2} - q_{i3} w_{i,j_3} \\ -q_{i0} w_{i,j_1} - q_{i1} w_{i,j_0} - q_{i2} w_{i,j_3} + q_{i3} w_{i,j_2} \\ -q_{i0} w_{i,j_2} + q_{i1} w_{i,j_3} - q_{i2} w_{i,j_0} - q_{i3} w_{i,j_1} \\ -q_{i0} w_{i,j_3} - q_{i1} w_{i,j_2} + q_{i2} w_{i,j_1} - q_{i3} w_{i,j_0} \end{bmatrix} \\
&= \sum_{i \in K} \begin{bmatrix} q_{i0} w_{i,j_0} - q_{i1} w_{i,j_1} - q_{i2} w_{i,j_2} - q_{i3} w_{i,j_3} \\ -(q_{i0} w_{i,j_1} + q_{i1} w_{i,j_0} + q_{i2} w_{i,j_3} - q_{i3} w_{i,j_2}) \\ -(q_{i0} w_{i,j_2} - q_{i1} w_{i,j_3} + q_{i2} w_{i,j_0} + q_{i3} w_{i,j_1}) \\ -(q_{i0} w_{i,j_3} + q_{i1} w_{i,j_2} - q_{i2} w_{i,j_1} + q_{i3} w_{i,j_0}) \end{bmatrix}.
\end{aligned}$$

Taking the rows of the output vector for the real part and the imaginary parts respectively, and using Equation (1) we obtain

$$\frac{\partial \mathcal{L}(a_j^{(l-1)})}{\partial a_j^{(l-1)}} = \sum_{i \in K} (q_i w_{i,j})^*$$

*B. Derivative with respect to the weights*

The derivative with respect to the layers weights  $w^{(l)}$  is calculated following

$$\begin{aligned}
\begin{bmatrix} \frac{\partial \mathcal{L}}{\partial w_0} \\ \frac{\partial \mathcal{L}}{\partial w_1} \\ \frac{\partial \mathcal{L}}{\partial w_2} \\ \frac{\partial \mathcal{L}}{\partial w_3} \end{bmatrix} &= \begin{bmatrix} \frac{\partial \mathcal{L}}{\partial z_0} \frac{\partial z_0}{\partial w_0} + \frac{\partial \mathcal{L}}{\partial z_1} \frac{\partial z_1}{\partial w_0} + \frac{\partial \mathcal{L}}{\partial z_2} \frac{\partial z_2}{\partial w_0} + \frac{\partial \mathcal{L}}{\partial z_3} \frac{\partial z_3}{\partial w_0} \\ \frac{\partial \mathcal{L}}{\partial z_0} \frac{\partial z_0}{\partial w_1} + \frac{\partial \mathcal{L}}{\partial z_1} \frac{\partial z_1}{\partial w_1} + \frac{\partial \mathcal{L}}{\partial z_2} \frac{\partial z_2}{\partial w_1} + \frac{\partial \mathcal{L}}{\partial z_3} \frac{\partial z_3}{\partial w_1} \\ \frac{\partial \mathcal{L}}{\partial z_0} \frac{\partial z_0}{\partial w_2} + \frac{\partial \mathcal{L}}{\partial z_1} \frac{\partial z_1}{\partial w_2} + \frac{\partial \mathcal{L}}{\partial z_2} \frac{\partial z_2}{\partial w_2} + \frac{\partial \mathcal{L}}{\partial z_3} \frac{\partial z_3}{\partial w_2} \\ \frac{\partial \mathcal{L}}{\partial z_0} \frac{\partial z_0}{\partial w_3} + \frac{\partial \mathcal{L}}{\partial z_1} \frac{\partial z_1}{\partial w_3} + \frac{\partial \mathcal{L}}{\partial z_2} \frac{\partial z_2}{\partial w_3} + \frac{\partial \mathcal{L}}{\partial z_3} \frac{\partial z_3}{\partial w_3} \end{bmatrix} \\
&= \begin{bmatrix} q_0 a_0 - q_1 a_1 - q_2 a_2 - q_3 a_3 \\ -q_0 a_1 - q_1 a_0 + q_2 a_3 - q_3 a_2 \\ -q_0 a_2 - q_1 a_3 - q_2 a_0 + q_3 a_1 \\ -q_0 a_3 + q_1 a_2 - q_2 a_1 - q_3 a_0 \end{bmatrix} \\
&= \begin{bmatrix} q_0 a_0 - (-q_1)(-a_1) - (-q_2)(-a_2) - (-q_3)(-a_3) \\ q_0(-a_1) + (-q_1)a_0 + (-q_2)(-a_3) - (-q_3)(-a_2) \\ q_0(-a_2) - (-q_1)(-a_3) + (-q_2)a_0 + (-q_3)(-a_1) \\ q_0(-a_3) + (-q_1)(-a_2) - (-q_2)(-a_1) + (-q_3)a_0 \end{bmatrix}.
\end{aligned}$$

Composing the rows back to a quaternion and using Equation (1) yields

$$\frac{\partial \mathcal{L}(w)}{\partial w^{(l)}} = q^* a^*.$$

*C. Derivative with respect to the bias*

As the respective bias component is not involved in the calculation of all output components, but just  $b_0$  for  $z_0$ ,  $b_1$  for  $z_1$ ,  $b_2$  for  $z_2$  and  $b_3$  for  $z_3$ , the derivatives simplify to

$$\begin{bmatrix} \frac{\partial \mathcal{L}}{\partial b_0} \\ \frac{\partial \mathcal{L}}{\partial b_1} \\ \frac{\partial \mathcal{L}}{\partial b_2} \\ \frac{\partial \mathcal{L}}{\partial b_3} \end{bmatrix} = \begin{bmatrix} \frac{\partial \mathcal{L}}{\partial z_0} \frac{\partial z_0}{\partial b_0} \\ \frac{\partial \mathcal{L}}{\partial z_1} \frac{\partial z_1}{\partial b_1} \\ \frac{\partial \mathcal{L}}{\partial z_2} \frac{\partial z_2}{\partial b_2} \\ \frac{\partial \mathcal{L}}{\partial z_3} \frac{\partial z_3}{\partial b_3} \end{bmatrix} = \begin{bmatrix} q_0 \\ -q_1 \\ -q_2 \\ -q_3 \end{bmatrix}.$$

Consequently, the conversion back to a quaternion is

$$\frac{\partial \mathcal{L}(b)}{\partial \mathfrak{b}^{(l)}} = q^*.$$